Durability of Chopped Fiber-Reinforced Polymeric Composites for use in Experimental Automotive Fuel Cells

By

James A. Fazio Jr.

Thesis submitted to the Faculty of the
Virginia Polytechnic Institute and State University
in partial fulfillment of the requirements for the degree of

Master of Science
in
Engineering Mechanics

John J. Lesko, Chair
Scott W. Case
B. K. Ahn

August 8, 2003
Blacksburg, Virginia

Keywords: Composite materials, Fuel Cells, fiber-reinforce polymer (FRP), pressure plate, chopped fiber composite, chemical durability, antifreeze, blisters

Durability of Chopped Fiber-Reinforced Polymeric Composites for use in Experimental Automotive Fuel Cells

James A Fazio Jr.

(ABSTRACT)

Recent interest in utilizing hydrogen fuel cell technology for automotive applications has lead to concerns regarding the durability of fiber reinforced polymer (FRP) composite materials. Automotive fuel cell power train systems must prove themselves as a reliable alternative to the combustion engines and automatic transmissions. The use of polymer composites in fuel cells to serve as manifolds is promising because of their high strength to weight ratio, and they do not corrode like metals manifolds. Composite materials designed for use in Polymer Electrolyte Membrane (PEM) Fuel Cells are exposed to very high humidity environment and operated at elevated temperatures (~85°C). The susceptibility of fiber reinforced polymers to reduction in modulus, strength, and life in chemical environments has been well documented in the literature, especially at elevated temperatures.

A chopped carbon fiber epoxy composite (Material A) and a chopped glass fiber epoxy composite (Material B) were exposed at 85°C to air, water, and a 50/50 water/antifreeze mixture, and periodically examined for tensile, compression, and flexural strengths at various temperatures. Following 2000 hours (83 days) of exposure, Materials A & B did not reach full saturation. Fatigue tests were conducted at various load levels and temperatures to determine their effect on cycles to failure, and carpet plots were generated. Blister formation in aged composites led to reductions in material properties as great as 25% to 75%. A mechanistic explanation was developed for the formation of blisters in the epoxy composite. Recommendations for material improvement and feasibility of material use for fuel cell manifolds and pressure plates were made.

Acknowledgments

The author would like to acknowledge the following for their contribution and support in this work:

- Dr. John “Jack” Lesko, for serving as my advisor and friend. Jack went out on a limb and gave me an opportunity that has changed my life. For this I will be forever grateful.

- Dr. Scott Case, for his patience and friendship. Scott has always there been to help and teach even when very busy. Dr. Case has helped me with so many problems it would be impossible to name them all.

- Dr. B. K. Ahn, for serving on my committee with such short notice and for his advice and friendship.

- Mac McCord, for his devoted service to the MRG. Not a single result on this project would have been possible without Mac’s help.

- Dr. Howard Halverson, for his help with testing and willingness to answer so many questions, especially when I first started with the MRG.

- Buzz, for his help with testing and for all of the great stories.

- Austin, for his help with testing and his patience when I began to lose all sanity.

- John Bausano, for his help, friendship, and ability to take a joke. It has kept me from going crazy on many days.

- Michael Hayes, for answering all of the questions that I should already know. May there always be “Good Times” for you.

- Materials Response Group for their support, their help, and their friendship.

- Beverly Williams, Sheila Collins, for making me feel at home since my first day in the MRG. Two smiling faces, who are always willing to help.

- Pat Baker, for putting up with all my nonsense and forgetfulness. Thank you for your patience.

- Bob Simonds, for his friendship, cycling knowledge, and help with so much of my research over the past two years. May you always keep the tire side down.

§ Dr. Nancy Love, for her friendship, guidance, and strength. Nancy is truly one of the greatest human beings to walk this planet. May you always find the time to swim, bike, and run…the papers and proposals can wait!

§ Ms. Denise Wingfield, for showing me that hard work pays off and there are endless opportunities if I am willing to put in the effort. And, for the adelgids.

§ Anna M. Sablik, for all the little things she does to help, her understanding, friendship, and patience. I could not have done this without you.

§ Jerry & Amy Frostick, for their friendship and keeping me well equipped for triathlon. Without this sport I would have never been interested in composites and I definitely would not have remained sane.

§ My Parents & Sister, for always pushing me to do my best, your financial support and your love.

§ A final word of thanks to the UTC Fuel Cells for providing me with the funding to support this research.

Table of Contents

List of Tables

List of Figures

Chapter 1: Introduction and Literature Review

1.1 Introduction

Recent interest in utilizing hydrogen fuel cell technology for automotive applications has lead to concern regarding the durability of fiber reinforced polymer (FRP) composite materials for such applications. Automotive fuel cell power train systems must prove themselves as a reliable alternative to the combustion engines and automatic transmissions. Durability concerns are focused on the environmental operating conditions of the fuel cells. Composite materials designed for use in Polymer Electrolyte Membrane Fuel Cells are exposed to a very high humidity environment and run at elevated temperatures. The susceptibility of fiber reinforced polymers to reduction in modulus, strength, and life in wet environments has been well documented in the literature, especially at elevated temperatures.

Polymer electrolyte membrane fuel cells (PEM), also know as proton exchange membrane fuel cells, are typically the fuel cell design chosen for applications in automobiles. A PEM fuel cell uses hydrogen and oxygen from the air to produce electricity through an electrochemical reaction (Figure 1). A single cell produces around 1 volt of electricity [1]. Therefore, several cells must be assembled in parallel to form a stack in order to produce enough energy to run a vehicle. Figure 2shows and example of a PEM fuel cell stack assembly.

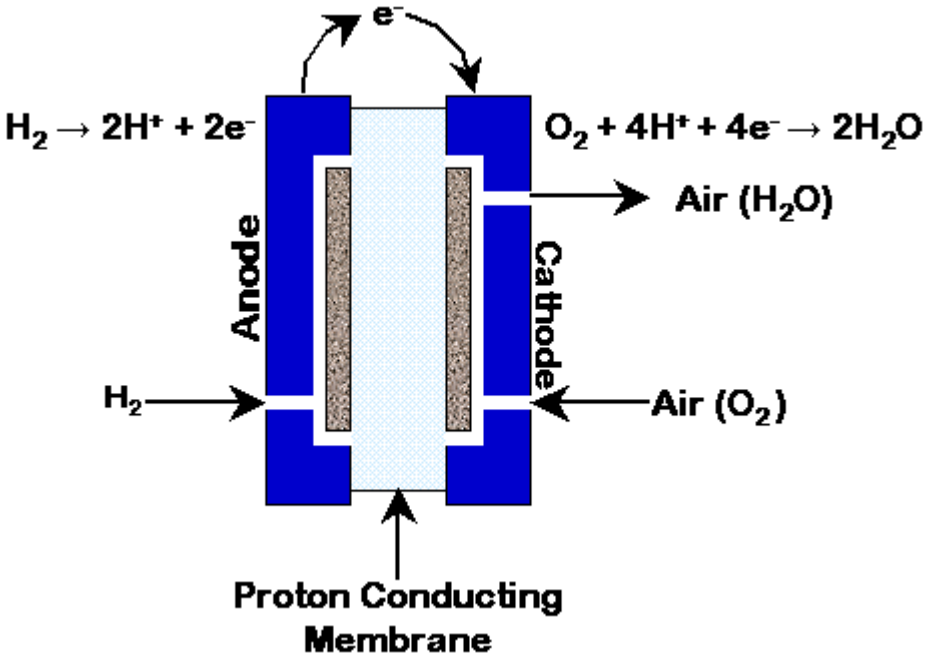

Figure 1: Design of a PEM fuel cell stack (Image courtesy of Lynntech, Inc.)[2]

These cells are held in place using composite manifolds and end pressure plates that form an impermeable sealed container. As part of the stack, the manifold system manages the gas and moisture flow. There are both internally manifolded, as well as, externally manifolded fuel cells.

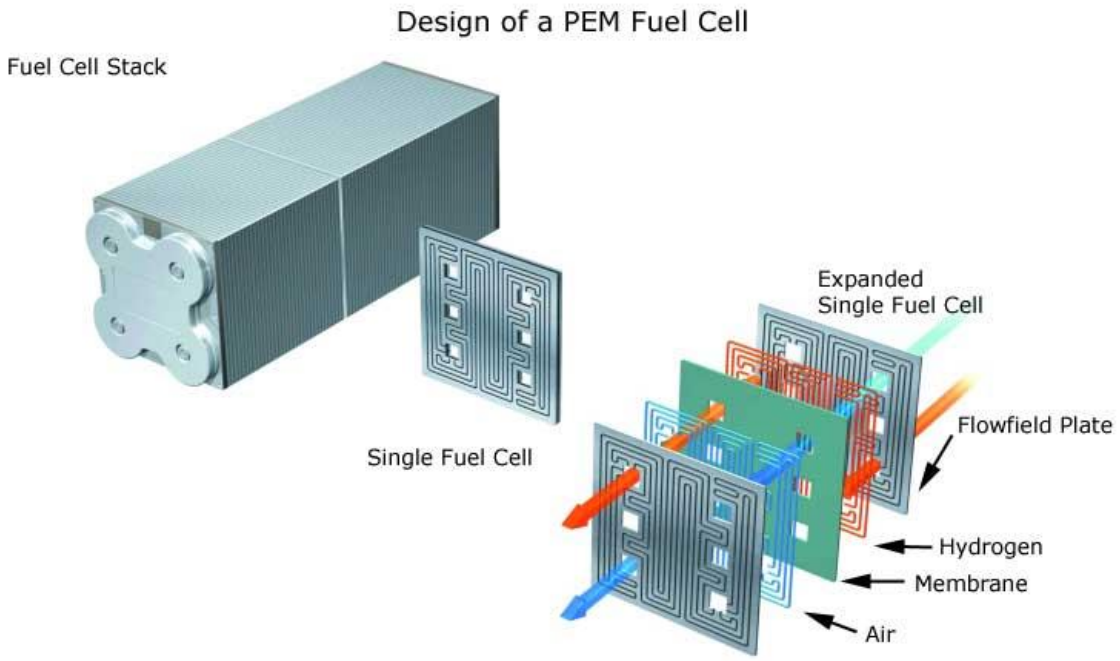

Figure 2: Design of a PEM fuel cell stack (Image courtesy of Ballard Power Systems) [3]

1.2 UTC Fuel Cell Manifolds and Pressure Plates

UTC Fuel Cell external manifolds and pressure plates are designed to channel the reactive gases and a 50/50 antifreeze/water cooling solution mixture, as well as, provide the high humidity environment required for efficient operation. The manifolds and pressure plates are exposed to a 100% humidity environment at elevated temperature. In addition to the moisture exposure due to high humidity, these components are exposed to a 50/50 mixture of water and ethylene glycol antifreeze. Very little data is available on the durability of FRPs exposed to antifreeze or antifreeze solutions. The manifolds and pressure plates will be exposed to various temperatures during operation, as well as thermal cycling due to startup and cool down just as a combustion engine endures when it is started up and turn off.

The material requirements are of the greatest concern in this study. The Department of Energy has set the goal of a 50% reduction of vehicle weight and vehicle subsystems for high volume production vehicles [4]. This requirement prompted the use of fiber reinforce polymers due to their reputation for having high stiffness- and strength-to-weight ratios compared to other materials. In addition to their weight advantages, FRP's are often declared to offer greater resistance to environmental degradation compared to the traditional engineering materials. The resistance to environmental degradation is paramount to meet the life requirement for PEM Fuel Cells, and is outlined below.

The department of energy characteristic requirement for the life of a transportation fuel cell system is fifteen years for a system capable of delivering at least 55 kW for eighteen seconds and a continuous power supply of 30 kW [5]. To meet this goal, the material components of the fuel cell stack must be durable enough to sustain all operating conditions with little degradation, thus preventing the contamination of the fuel cell. The material components include the manifolds and pressure plates described above.

The exposure of the manifolds and pressure plates to various solutions during operation is a concern. Exposure to water and the mixture of water and ethylene glycol antifreeze has the potential to degrade these components over time. The current design of the manifold requires the FRP manifold to be in direct contact with both pure water and a 50/50 water/ethylene glycol antifreeze solution used for cooling the fuel cell.

The typical operating temperature for a PEM fuel cell is approximately 80° Celsius [1]. A byproduct of the reaction that occurs in a PEM fuel cell is heat. In order to maintain the operating temperature, a cooling system is required. The material components of the fuel cell, as well as, the cooling solution within the stack must be stable at this elevated temperature for long periods of time.

An addition temperature related concern involves the thermo-cycling of the fuel cell. For automotive applications, the fuel cell must operate in temperature ranges from a cold start up as low as -20° Celsius to an operating temperature as great as 85° Celsius. The materials must be capable of withstanding stresses associated with this type of thermo cycling.

1.3 Literature Review

1.3.1 Moisture Degradation

The effects of moisture absorption on mechanical properties of FRP composites have been well documented in the literature. The durability of FRP composites in moist environments is directly related to the performance of the fibers, matrix, and interface of the composite. The amount of solvent that penetrates the composite is dependent upon both time, temperature, material type, and solvent type [6].

Fiber

Carbon fibers are largely unaffected by moisture; their glass counterparts are not as durable. The performance of silica and silicate glasses exposed to aqueous environments has been shown to degrade as a result of dissolution, selective leaching, and stress-corrosion cracking [7]. Diffusion, as well as, hydrolysis and condensation reactions are the primary methods for water induced damage to the glass surface [8]. McKinnis [9] suggests that applying a stress to the fiber increases the moisture concentration on the fiber. This study also proposed that the rate of diffusion of water into the glass structure is primarily controlled by the size of the voids present in the glass network. Bunker [7] reported that the voids in most glass structures are too small to allow diffusion, and therefore, the dissolution of most glasses is due to semi-reversible hydrolysis and condensation reactions (although these reactions are not completely reversible). Several studies found that the strength of glass fibers is controlled by a stress corrosion reaction that occurs when water diffuses to the fiber surface inducing a micro-flaw which leads to fiber fracture. This is especially prevalent for conditions in which the

fiber is stressed [9-10]. An essential part of this stress corrosion reaction is the ionic exchange of sodium in the glass with available hydrogen ions leading to a reduction in glass volume [11,7]. The hydrogen ion is significantly smaller then the sodium ion it replaces forming void space that allows for further diffusion of water and the propagation of cracks toward the center of the fiber [12]. This process is highly dependent upon the glass structure; however there is considerable evidence that the adsorption of water to the glass is the rate controlling step [7]. Each of the damage mechanisms is important when considering composites exposed to aqueous environments.

The Epoxy Matrix

While Bunker [7] suggested that the rate-limiting step in glass fiber damage was water adsorption to glass, the water must first penetrate the epoxy matrix in order to contact the fiber in a composite. The moisture absorption characteristics of an epoxy matrix are dependent upon the stoichiometry corresponding to the amounts of epoxy and amine curing agent. Moisture saturation levels and diffusivities are considerably affected by the concentrations of epoxy and amine curing agent [13]. Due to the proprietary nature of many resin systems used in composite materials, stoichiometries are not always known.

Significant literature focuses on the interaction of water molecules within a polymer system and the corresponding changes in the epoxy network microstructure. Adamson [14] showed water molecules interact in two ways with epoxy. The "un-bound" water molecules can cluster within the free volume of the epoxy, and the "bound" molecules form hydrogen bonds with hydrophilic groups in the epoxy. These hydrogen bonded molecules are responsible for matrix swelling. The non-hydrogen bonded molecules can permeate through the free volume of the epoxy. Zhou and Lucas [15] determined that the hydrogen bonding between the water molecules and the epoxy resin network occurs in two forms. The first is the formation of a single hydrogen bond between the water molecule and the epoxy. In this case the water acts as a plasticizer. This effect is likely to reduce the stiffness and brittleness of the epoxy, therefore leading to a lower glass transition temperature (T_g) for the epoxy. Zhou and Lucas [16] showed in the second part of their study that both forms of hydrogen bonding affect the glass transition temperature. The single hydrogen bonded water molecule causes a reduction in T_g. In the case in which the water molecules form multiple hydrogen bonds within the epoxy matrix, a corresponding increase in the glass transition temperature occurs due to the secondary cross linking formed by the hydrogen bonded water molecules. This damage to the network reduces the molecular weight of the epoxy polymer chain. These changes in the microstructure of the epoxy system are likely to cause damage to the interface between the epoxy matrix and structural fiber.

The Fiber/Matrix Interface

With both the fibers and the matrix affected by the absorption of moisture, it is essential to examine the fiber/matrix interface. As stated above, the moisture absorption into matrix causes a reduction in the glass transition temperature of the epoxy system. This reduction in T_g reduces the strength of the fiber/epoxy interface [13,17]. The failure of composites at saturated conditions is due to degradation at the interface rather than changes in matrix mechanical properties resulting from water absorption in the matrix [17, 18]. Another study, using single fiber fragmentation tests on an E-glass/Epoxy

composites, found that the strengths of the fibers and the fiber/matrix interface were shown to decrease after immersion in water [19].

Chopped Fiber Reinforced Epoxy

Fiber arrangement has a substantial effect on the composite moisture absorption. Singh, Singh, and Rao [20] found that chopped fiber composites have greater diffusivities then woven roving composites, especially when the chopped fiber is in the top layer (first to be exposed to the moisture) of a laminate. In general, laminates with chopped fibers tend to have lower fiber volume fractions than laminates with woven roving fibers. Equilibrium moisture levels tend to be higher in composites with lower fiber volume fraction [20-21].

1.3.2 Antifreeze Degradation

As detailed above, there is extensive literature into the degradation of mechanical properties and moisture absorption in fiber reinforced epoxies. However, very little information is available regarding the durability of epoxy composites to ethylene glycol antifreeze. A study on automotive parts showed that Bisphenol-A Epoxy underwent a 60% reduction in flexural strength following a three week exposure to a 50/50 water/ethylene glycol antifreeze mixture [22]. The temperature at which this study was conducted was not stated. It is unclear whether the reduction in flexural strength is due to the absorption of water or chemical attack from contact with the ethylene glycol.

Springer [23] examined the effects of antifreeze at different temperatures on polyester and vinylester composites. For polyester resins with a high amount of calcium carbonate filler, significant decreases in tensile strength, short beam shear strength, and short beam shear modulus were shown after 180 days aging in 93°C antifreeze. Tensile modulus showed little change between 30 and 180 days of aging. Polyester resin with low amounts of filler experienced extreme reductions in tensile strength, tensile modulus, short beam shear strength, and short beam shear modulus. The vinyl ester matrix composite saw limited loss in tensile strength and tensile modulus, but greater losses in short beam shear strength and short beam shear modulus.

1.3.3 Temperature Concerns

As mentioned above, a PEM fuel cell has an operating temperature around 80°C. In colder environments it is very possible that the cells could also be exposed to temperature well below freezing (-40°C). This is a wide range of temperatures and the thermal effects associated with this range are of concern. As with moisture, the fibers, matrix, and fiber/matrix interface can all be affected. Understanding the effect of temperature on each of the fuel cell components allows for improvements in design and materials choice or processing.

Fiber

The operating temperatures of a PEM fuel cell are not extreme enough to directly cause fiber damage. However, temperature does affect the amount of moisture within a composite. Evidence of the temperature dependence of moisture induced damage was shown by Metcalfe and Schmitz [11]. The researchers concluded that extreme-cold inhibits stress corrosion of glass fibers by limiting the amount of available moisture to initiate damage. In line with the findings of Metcalfe and Schmitz, McKinnis [9] concluded that only microstress-surface sorbed water is destructive at lower

temperatures. While cold temperatures may reduce the damage to glass fibers resulting from moisture attack, room temperature and elevated temperatures offer no protection.

The Epoxy Matrix

The effects of temperature on the epoxy matrix are dependent upon the stoichiometry of the epoxy and the hardening agent. The stoichiometry, as well as, post curing affect on the glass transition temperature of the material and therefore its response to temperature changes. Gupta *et al.* [24] examined some mechanical properties of an epoxy system at several stoichiometries at various temperatures. They observed large decreases in stiffness and yield point as temperature increased for samples with low glass transition temperatures. In addition, for epoxies with low molecular weight and low T_g, it was found that a rapid decrease in tensile strength occurs with an increase in temperature.

Temperature is also a controlling element in the mechanism of moisture absorption in the epoxy matrix. As has been well documented in the literature, an increase in exposure temperature corresponds to an increase in non-Fickian behavior [13, 25]. In addition, the total amount of moisture absorbed is dependant upon temperature; the absorbed moisture is greater at higher temperatures [6].

The Fiber/Matrix Interface

Several studies in the literature have examined the effects of temperature on the fiber/matrix interface. One such study found that at temperatures lower then the bulk matrix glass transition temperature, there was significant increase in the critical aspect ratio of the composite [26]. The authors of this study suspected that the increase in aspect ratio is due to small disturbances at the interface. This increase may explain why critical length is dependent on temperature.

1.3.4 Composite Durability

The durability of a fiber reinforced polymer composite is dependent upon the durability of each of its components. The degradation mechanisms for each component discussed above can help one understand their interaction as a system. The PEM fuel cell manifolds and pressure plates this study is concerned with are a chopped fiber reinforced epoxy. Substantial literature is available on the effects of temperature and moisture on the mechanical properties fiber reinforced epoxy composites.

Chopped fiber reinforced composites tend to have lower fiber volume fractions. As mentioned earlier, composites with low fiber volume fractions tend to have a higher equilibrium moisture level. This elevated moisture level undoubtedly affects the durability of the composite in moist environments because of its damaging effects on the fibers, matrix, and fiber/matrix interface. It has been shown that the strength and stiffness of chopped glass fiber epoxies are reduced when exposed to moisture [20]. The authors of this study attributed the reductions to moisture-induced swelling and plasticization leading to delamination. They also concluded that the shear strength of the composites decreased with increasing temperature and time of exposure to moisture.

In a separate study of composites with woven roving laminates, cross-ply $[0_2,90_3]_s$, multi-directional $[\pm45, 90_3]_s$, and angle-ply $[\pm45]_s$, researchers found that glass-fiber/epoxy composite laminates absorb moisture and swell when immersed in distilled water [27]. In this study Ellyin and Rohrbacher also found that temperature of the water the specimens were immersed in controlled the amount of water absorbed into the composites. Samples aged at 90°C formed blisters and matrix cracks. The degradation

resulted in the decrease of fatigue strengths from 38% to 65 % compared to dry specimens.

Several other studies have shown mechanical properties reductions in glass reinforced epoxy composites. Beehag and Ye [28] observed a 20% reduction in burst strength of a glass/epoxy filament-wound tube following the absorption of 1.5% by weight seawater. In another study, it was observed that tensile strength and failure strain were reduced by more then 50% following submersion in boiling water [29].

Carbon fiber reinforced epoxies are also susceptible to damage. Zhou and Lucas [25] concluded that absorbed water in a graphite epoxy composite is concentrated at crack tips, interfaces and voids when aged at elevated temperatures. They also observed behavior consistent with moisture absorption of neat epoxy. In another study, researchers observed up to a 17% reduction in transverse tensile strength due to moisture absorption [30]. The authors concluded that this strength loss was associated with degradation of the interface, and also stated that the fracture mechanism changes from matrix cracking to interfacial failure under these conditions.

1.4 Problem Statement

As PEM fuel cell powered automobiles are going into limited production, there are concerns about the durability of the fuel cells and their components. Each component must be tested to determine its durability in the same environment it will be exposed to as a component of the fuel cell. The chopped fiber reinforced epoxy under investigation for use in fuel cell manifolds and pressure plates is exposed to temperatures ranging from -40°C to 85°C. This material is also exposed to water and ethylene glycol antifreeze at these temperatures. With a reliable life requirement of fifteen years, the materials will be subjected to moisture, thermal, chemical, and their combined effects for long periods of time.

To evaluate the durability of this material, a simulated aging environment has been developed. The composite materials are exposed to service like conditions and periodically examined for tensile, compression, and flexural strengths at various temperatures. Moisture uptake was conducted during the aging period. Fatigue of the material was conducted at various load levels and temperatures to determine their effect on cycles to failure. Analysis of strength, fatigue, and damage mechanisms were conducted and recommendations for improvement of mechanical properties were made.

Chapter 2: Materials and Methods

2.1 Materials System

This study examines the degradation of mechanical properties of two composites used by UTC Fuel cells. These materials have been selected for use in composite manifolds and end pressure plates for a PEM fuel cell. Material A is a chopped carbon fiber reinforced Epoxy. Material B is a chopped glass fiber reinforced Epoxy. Typical properties provided by the manufacturer for Material A and Material B are shown in Table 1 and Table 2 respectively [31].

Table 1. Manufacturer's Reported Properties for Material A

Material A	
Reinforcement % by weight	55%
Reinforcement % by volume	52%
Reinforcement Length	1" 3k
Reinforcement type	chopped carbon
Specific Gravity grams/ cc	1.45
Density lbs./cu. in.	0.0524
Polymeric Shrinkage in./in.	0
Flexural Strength D-790 psi	89,000
Flexural Modulus D-790 psi x 10^6	5
Tensile Strength D-638 psi	42,000
Tensile Modulus D-680 psi x 10^6	8
Comp. Strength D-695 psi	40,000
Comp. Modulus D-695 psi x 10^6	4.6
Notched Izod D-256 ft-lbs/in	18
Poison's Ratio	0.5
Tg, DMA D-4065	347° F

Table 2. Manufacturer's Reported Properties for Material B

Material B	
Reinforcement % by weight	63%
Reinforcement % by volume	45%
Reinforcement Length	1/2"
Reinforcement type	chopped glass
Specific Gravity grams/ cc	1.82
Density lbs./cu. in.	0.0658
Polymeric Shrinkage in./in.	0.001
Flexural Strength D-790 psi	66,000
Flexural Modulus D-790 psi x 10^6	2.6
Tensile Strength D-638 psi	35,000
Tensile Modulus D-680 psi x 10^6	2.3
Comp. Strength D-695 psi	25,000
Comp. Modulus D-695 psi x 10^6	1.9
Notched Izod D-256 ft-lbs/in	35
Poison's Ratio	0.3
Tg, DMA D-4065	347° F

2.2 Specimen Preparation for Aging

Composite panels manufactured by Quantum Composites measuring 12-inches x 12-inches x 1/8-inches were cut using a wet diamond saw to panels 5-inches wide by 6-inches long for aging. Each panel was labeled using a hand engraver in the top right corner. A random sample of panels were selected and used for the moisture uptake study. These specimens were individually weighed before insertion into the aging containers. Specimens were arranged radially using custom designed 15 cm clamping in PTFE (Teflon®) racks, fabricated from ½ inch thick Teflon® sheets, rods and nylon set screw collars, to ensure sufficient and equal access to moisture on all sides (Figure 3). The panels were then aged at 85° C in air, deionized water, and a 50/50 mixture of deionized water and ethylene glycol antifreeze for 1, 2, 4, 16, 32, or 83 days. A photo of the specimens in the water aging system is shown in Figure 4.

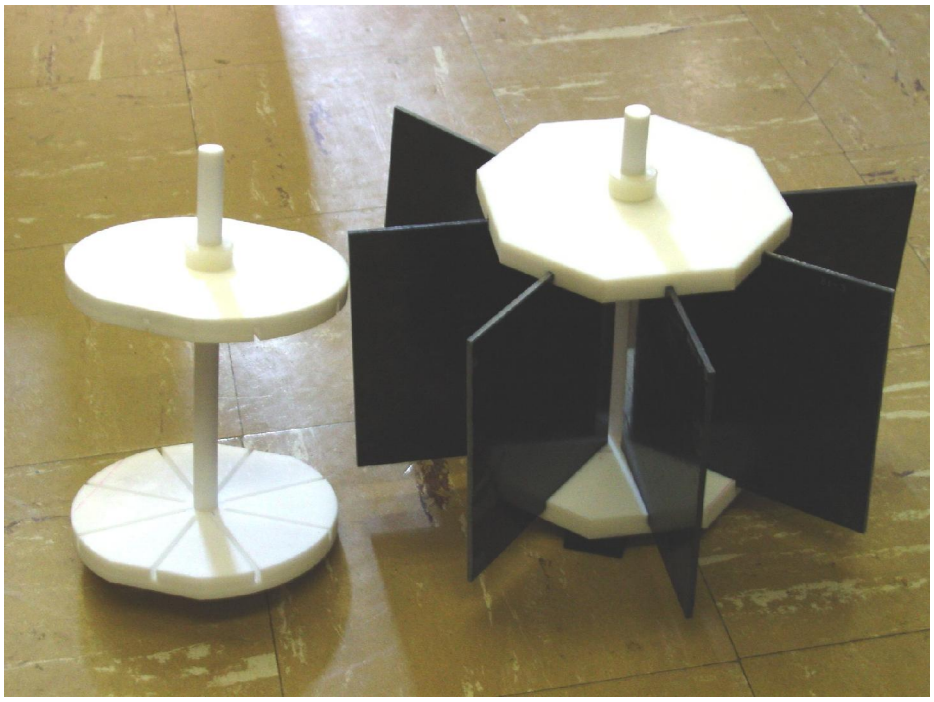

Figure 3: Radial Specimen Holders

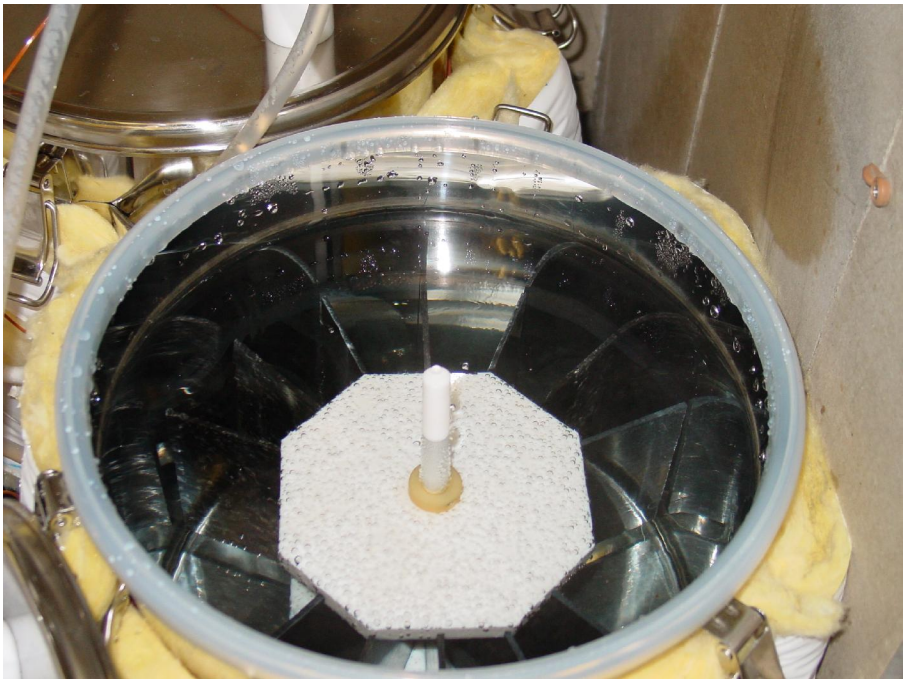

Figure 4: Samples inside water aging container

2.3 Aging System

The aging system containers are Eagle Stainless Container CTH-30 made of 316L Stainless Steel with a Platinum Cured Silicone rubber gasket and a 24 Ra standard finish

(15 Ra electro-polished). The containers were heated using 76 cm long flexible silicone rubber fiberglass insulated heater with a watt density of 5 W/in^2 from Omega Engineering, Inc. model number SRFG-1030/5. The heaters were attached using two wrappings of ½ inch hanger iron. A modified water heater blanket utilizing fiberglass insulation (R-19) was used as insulation for each container. Temperature control was performed using an Omega Subminiature quick-disconnect probe, type-K, 0.125" O.D. stainless steel sheath, grounded junction, 6" length (KMQSS-125G-6) thermocouple and Omega Controller. The condensers used were Kuhler 400mm Reflux condensers each having an internal coil that was water jacketed (Figure 5). Vapors are condensed both on the coil and the inner wall of the jacket. The condenser connection to the stainless steel lid of the aging container was made using a machined female, Teflon® tapered joint (29/42) attached to the container lid using 316 SS sheet metal screws (Figure 6). The condensers were supported using tension rods placed between the walls of the fume hood. The above described system can be seen in Figure 7. Air aging was conducted in an Espec ESX-4CA hygro-thermal cycling chamber (Figure 8).

Figure 5: Vapor Condensers with cooling water tubes

Figure 6: Teflon® connects for vapor condensers

Figure 7: Liquid aging system

Figure 8: Espec ESX-4CA hygro-thermal cycling chamber

2.4 Moisture Uptake Monitoring

Moisture uptake monitoring was performed in accordance with ASTM D5229-98 for Procedure A (Test Method for Moisture Absorption Properties and Equilibrium Conditioning of Polymer Matrix Composite Materials). The specimens were taken out of the tank and set into a cold bucket of water in order to slow outward diffusion of fluid during the moisture reading. The specimens were then wiped dry and placed on a Mettler AE 200 balance. The percent moisture uptake was measured using the following equation:

$$\%M = \frac{(Wx - Wo)}{Wo} * 100 \qquad \text{Equation 1}$$

Where:

Wx = wet weight at time x
Wo = dry weight at a time of 0
%M = percent moisture uptake

2.5 Specimen Preparation for Testing

On the day of testing, the panels were removed and cut into 5/8-inch wide by 6-inch long test specimens using a wet diamond saw. The edges of the specimens were lightly ground with 240-grit and 400-grit sandpaper to remove the diamond saw blade

marks. The specimens were labeled and measured using calipers to determine cross sectional area. The specimens were then sealed in a zip-lock bag and a wet paper towel was added if the specimens were aged in liquid. Since the specimens are tested within a couple of hours of preparation, moisture loss was assumed to be negligible.

2.5.1 Specimen Preparation for Testing

Cross sections of materials were cut for micro-photography. The samples were cut to approximately one-half to three-quarters of an inch in length and placed in standard 1.25" diameter metallographic mounts. Careful attention was paid to the alignment of the sample so that the cut cross-sectional area was parallel with the surface to be polished. The specimens were mounted in a two-part epoxy supplied by Buehler and cured overnight. In an effort to obtain the best possible polish of the surface, the epoxy was mixed extensively until homogeneous and with little creation of air bubbles.

Polishing was performed using a Buehler® Ecomet® 3 polisher with an Automet® 2 automatic head and silicon carbide sandpaper from 320 to 800 grit. Excess epoxy was removed prior to polishing with 100 grit sandpaper to ensuring the sample is exposed for polishing.

2.5.2 Quasi Static Testing

Quasi-static tensile tests were conducted using a servo-hydraulic load frame (MTS 20 kip capacity) operated in load control using a MTS 407 controller. For specimens tested in tension at 85°C the test machine was fitted with a custom designed, forced convection oven with temperature control provided by an Omega temperature controller (Figure 9). For tensile specimens tested at -20°C, a test machine was encased within a custom Russell self-controlled hygro-thermal environmental chamber that provided temperature regulation at -20°C (Figure 10). The specimens were loaded at a rate of 2000 lbs/min until failure. Strain data was recorded using an extensometer. Ultimate tensile strength and modulus were determined for each specimen.

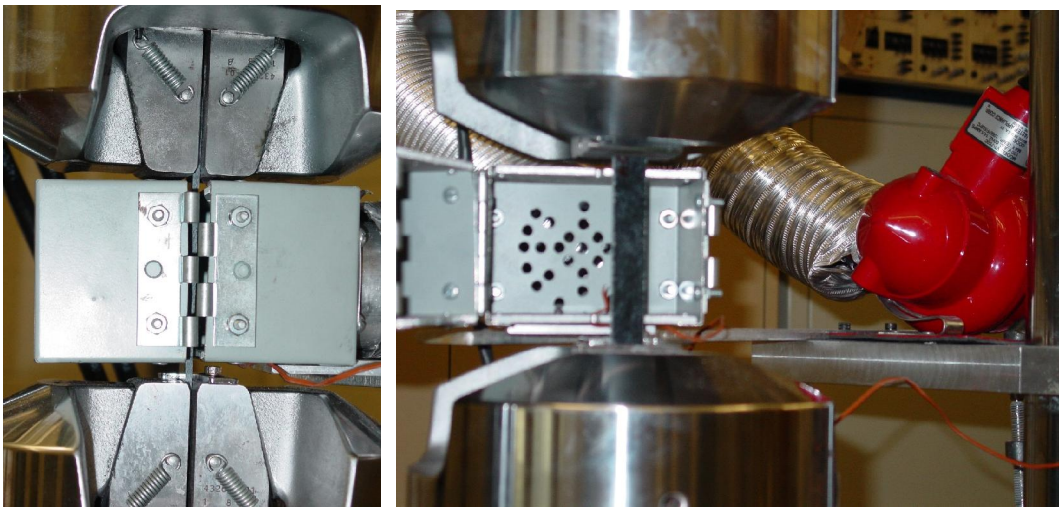

Figure 9: Custom designed, forced-convection oven

Quasi-static compression tests were conducted using a hydraulic driven, load driven MTS machine (20 kip capacity) controlled using a MTS 407 controller. The test machine was encased within a custom Russell self-controlled hygro-thermal environmental chamber that provided temperature regulation at 85°C and -20°C (Figure 10). The specimens were loaded at a rate of 1000 lbs/min until failure.

Figure 10: Environmental Chamber encased MTS test machine

The proposed test matrix for baseline static strength and stiffness data on Materials A and B are given in Table 3. Five tensile replicates and five compression replicates of each material for each aging condition (air, water, & antifreeze) as marked were tested. The tensile and compression test results were used to identify aging influence on mechanical properties, and the minimum necessary inputs for durability testing.

Table 3: Test Matrix for Baseline Static Strength and Stiffness

	85°C	Room Temp	-20°C
As Received	5	5	5
Aged 1 Day	5		
Aged 2 Days	5		
Aged 4 Days	5		
Aged 16 Days	5		
Aged 32 Days	5	5	5
Aged 83 Days	5	5	5

2.6 Flexural Strength Testing

Flexural strength testing was conducted in accordance with ASTM D 790-00. Flexural testing was conducted using an Instron 4204 screw driven test machine with a 5 kN load cell. The test matrix for flexural data on Materials A and B are given in Table 4. Five flexural replicates of each material for each aging condition (air, water, & antifreeze) as marked were tested.

Table 4: Flexural Strength Testing Plan

	85°C	Room Temp	-20°C
As Received		5	
Aged 32 Days		5	
Aged 83 Days		5	

2.7 Fatigue Testing

Fatigue tests were conducted using a hydraulic driven, load driven MTS machine (20 kip capacity) controlled using a MTS 407 controller. Specimens were loaded at a frequency of 10 Hz using a sinusoidal waveform. For specimens tested in tension at 85°C the test machine was fitted with a custom designed, forced convection oven with temperature control provided by an Omega temperature controller (Figure 6). For tensile specimens tested at -20°C, a test machine was encased within a custom Russell self-controlled hygro-thermal environmental chamber that provided temperature regulation at -20°C (Figure 10). Strain data was recorded using an extensometer for room temperature tests. A S/N curve was created for each material.

Fatigue compression tests were conducted using a hydraulic driven, load controlled MTS machine (20 kip capacity) regulated using a MTS 407 controller. The test machine was encased within a custom Russell self-controlled hygro-thermal environmental chamber that provided temperature regulation at 85°C and -20°C (Figure 10). An S/N curve was created for each material.

Test conditions examined are shown in Table 5. At each condition labeled with an asterisk, 5 replicate tests at 3 stress levels were conducted.

Table 5: R-ratio and Temperature Conditions Considered

R-ratio	85°C	Room Temp	-20°C
∞	*	*	*
Xt/Xc	*		
-1	*	*	*
-Xc/Xt	*		
0	*	*	*

Using the results from the developed S/N curves, "carpet" fatigue lifetime plots were produced for the mean stress values.

Chapter 3: Results and Discussion

Moisture uptake, quasi-static tensile and compression testing, as well as fatigue testing were conducted to determine the effects of the aging conditions on the test materials. The results of these tests are discussed below in detail.

3.1 Moisture Uptake

Percent moisture uptake was measured for Materials A and B in water and the 50/50 water/antifreeze mixture. The moisture uptake for both materials aged in 85°C deionized water is shown in Figure 11. The percent moisture uptake curve for these materials aged in the 50/50 water/antifreeze mixture is shown in Figure 12.

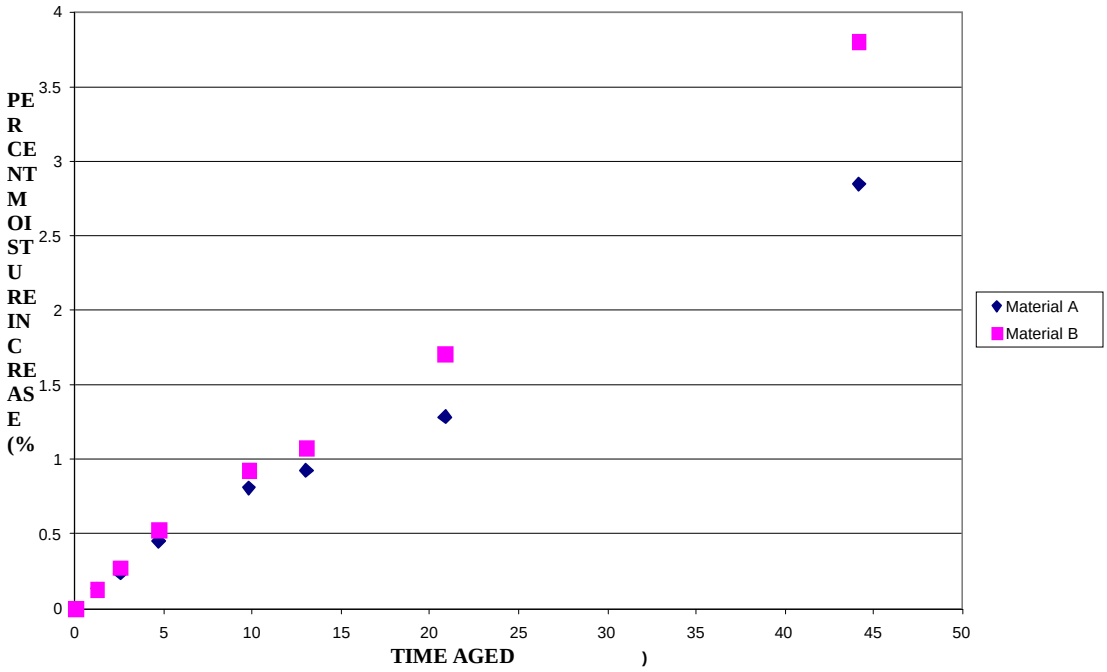

Figure 11: Percent Moisture Uptake for Materials A and B aged in 85°C Deionized Water

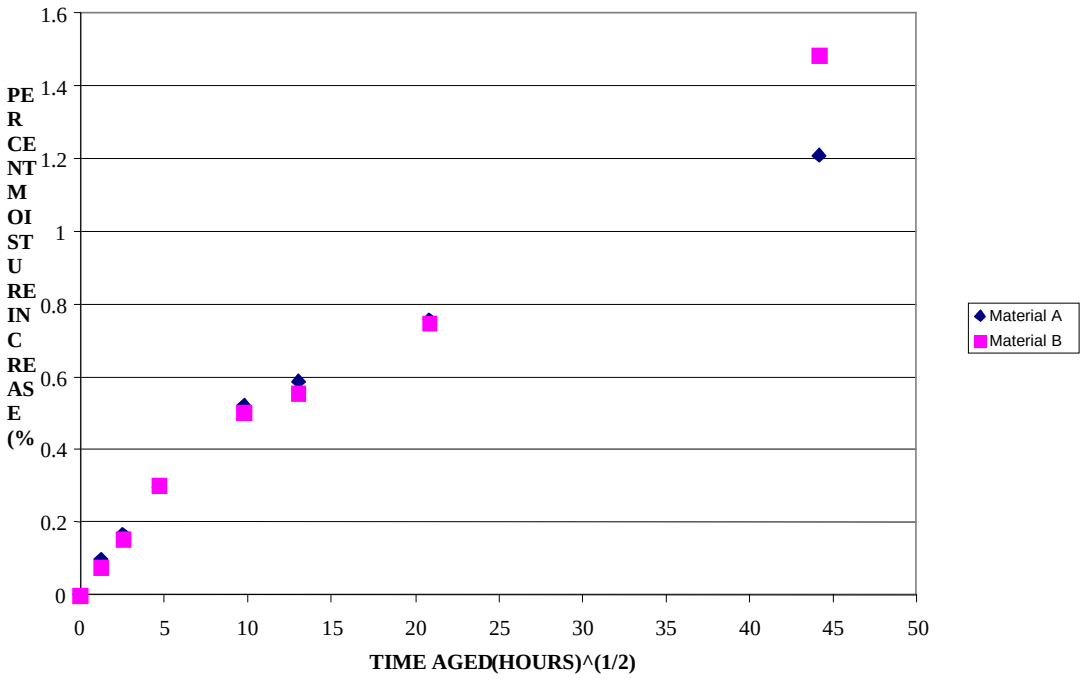

Figure 12: Percent Moisture Uptake for Materials A and B aged in 85°C 50/50 Mixture

The moisture absorption results for Materials A and B in both the water and the 50/50 water/antifreeze mixture exhibit non-Fickian behavior. In both cases, there appears to be a slight knee in the data around 100 hours of aging. Following this point we would expect a decrease in the moisture absorption rate far greater then what has been seen. Diffusion coefficients were not computed, as an M_∞ could not be determined. The continued increase in moisture absorption is likely due to internal delamination of the material and the formation of blisters in which water can continue to be stored as unbound water. Evidence of this mechanism can be observed in Figure 13, which compares the surfaces of Material A as received and after 83 days of aging. These samples were aged in 85°C deionized water. A comparison of Material B from 2 days aged through 83 days aged is shown in Figure 14. Micro-photographs were taken of cut cross sections of the material for as received, 2, 4, 16, 32, and 83 day water aged samples. A series of micro-photographs showing blister formation are shown in Figure 15.

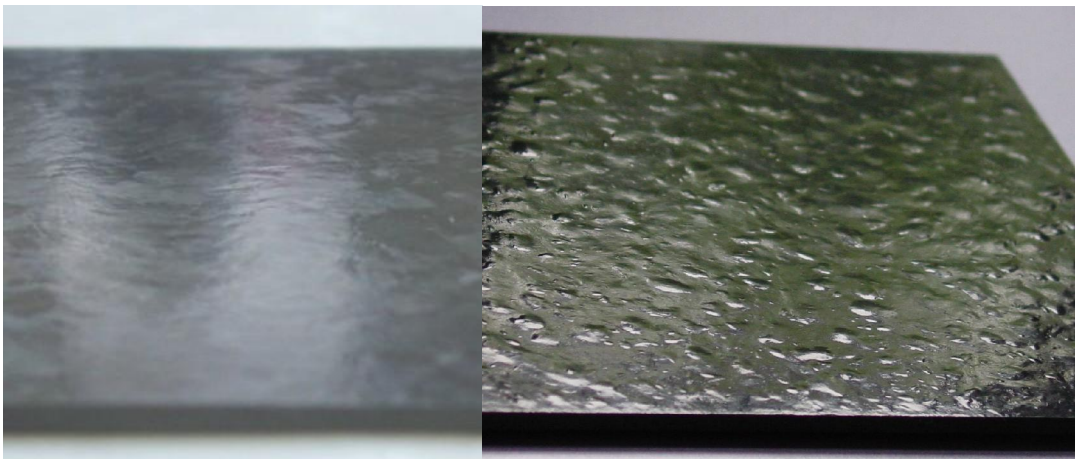

Figure 13: As received Material A (left) & 83 day 85°C water aged Material A (right)

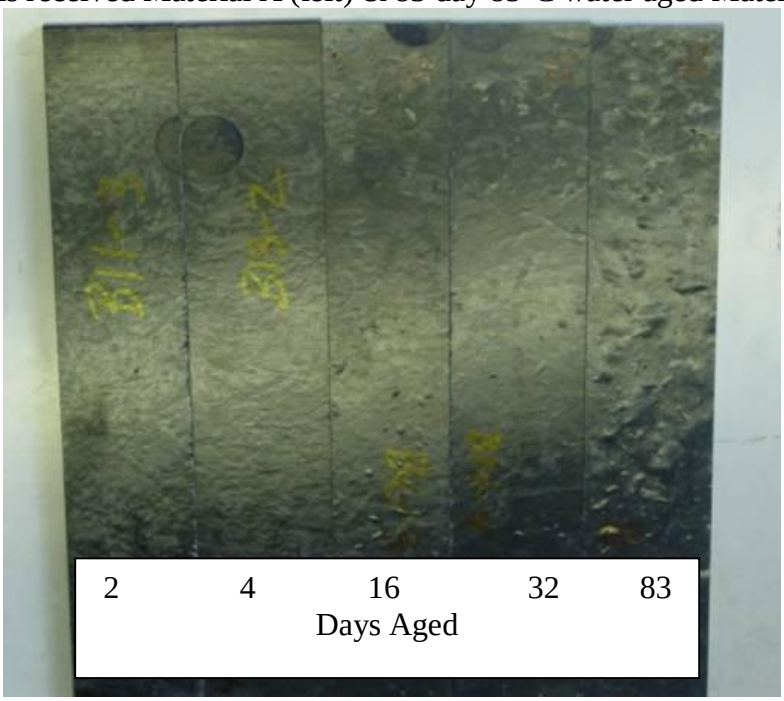

Figure 14: Material B 85°C water aged

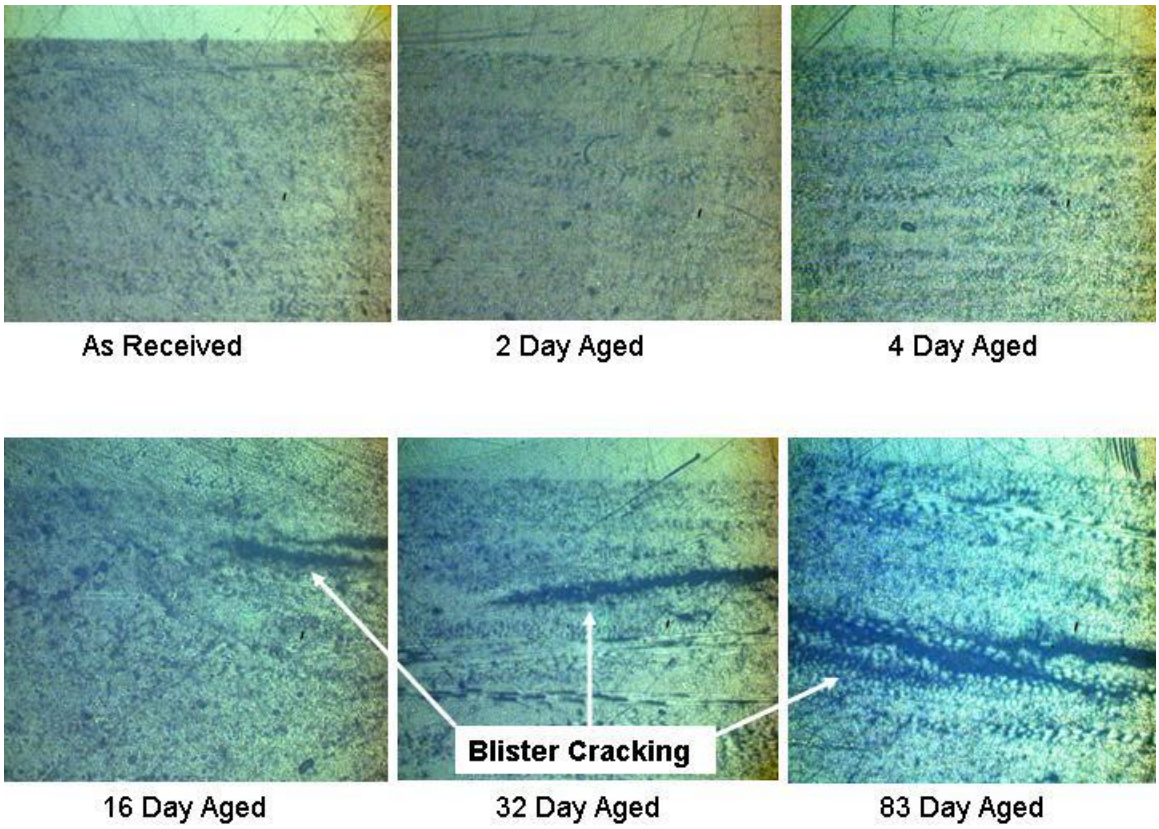

Figure 15: Cross-sectional micro-photographs of blister formation (Magnification 10X)

Although the damage was less severe in specimens aged in the antifreeze mixture (not shown), there was some delamination and blistering. The difference in degree of damage between the water and the water/antifreeze mixture is believed to be due to the lower concentration of water in the mixture. With only 50% of the mixture being water, there is less water available to penetrate the composite and induce damage.

3.2 Quasi Static Testing

3.2.1 Tensile Testing

A set of five replicate quasi-static tensile tests for each aging condition (air, water, 50/50 water/antifreeze mixture) were conducted for each of the composites Materials A and B for the as received, 1, 2, 4, 16, 32, and 83 days aged conditions. A typical tensile failure can be seen in Figure 16. The failures occur perpendicular to the load direction within the 3 inch heated gage section. Figure 17 and Figure 18 show the changes in average tensile strength versus time for the Materials A and B materials respectively.

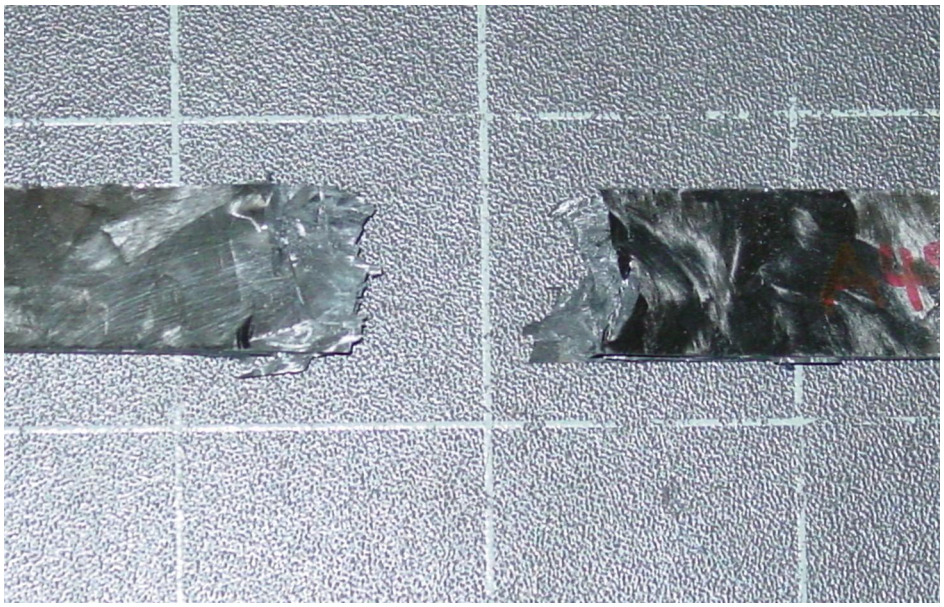

Figure 16: Typical tensile failure for Material A

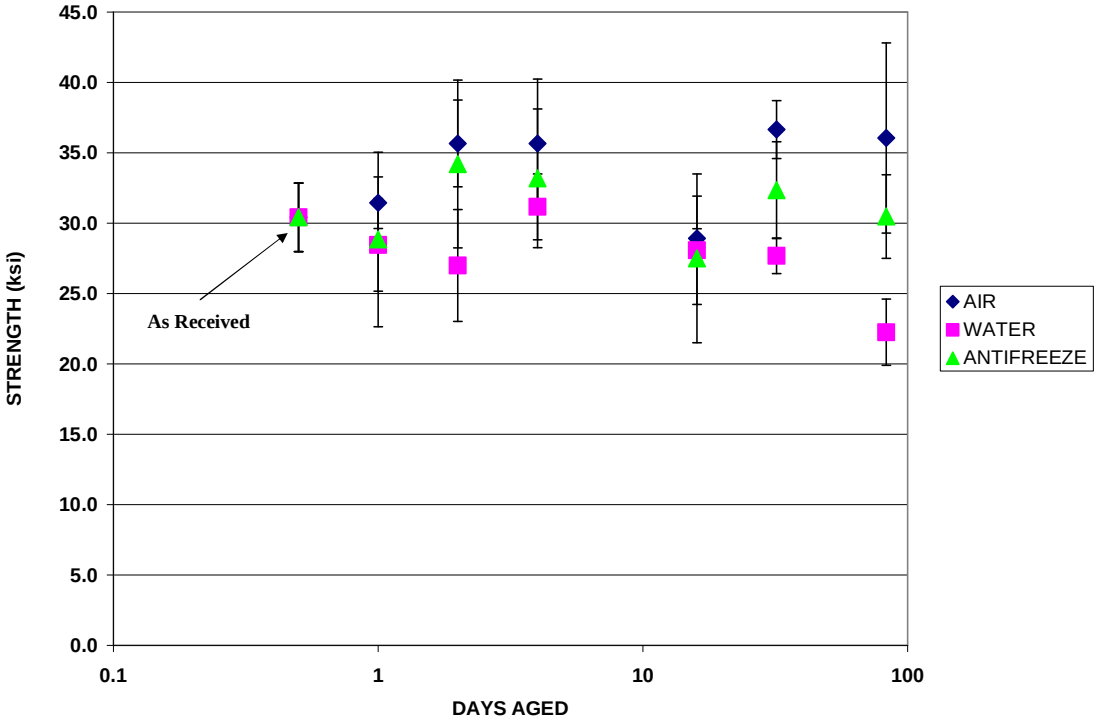

Figure 17: Materials A Tensile Strength vs. Aging Time

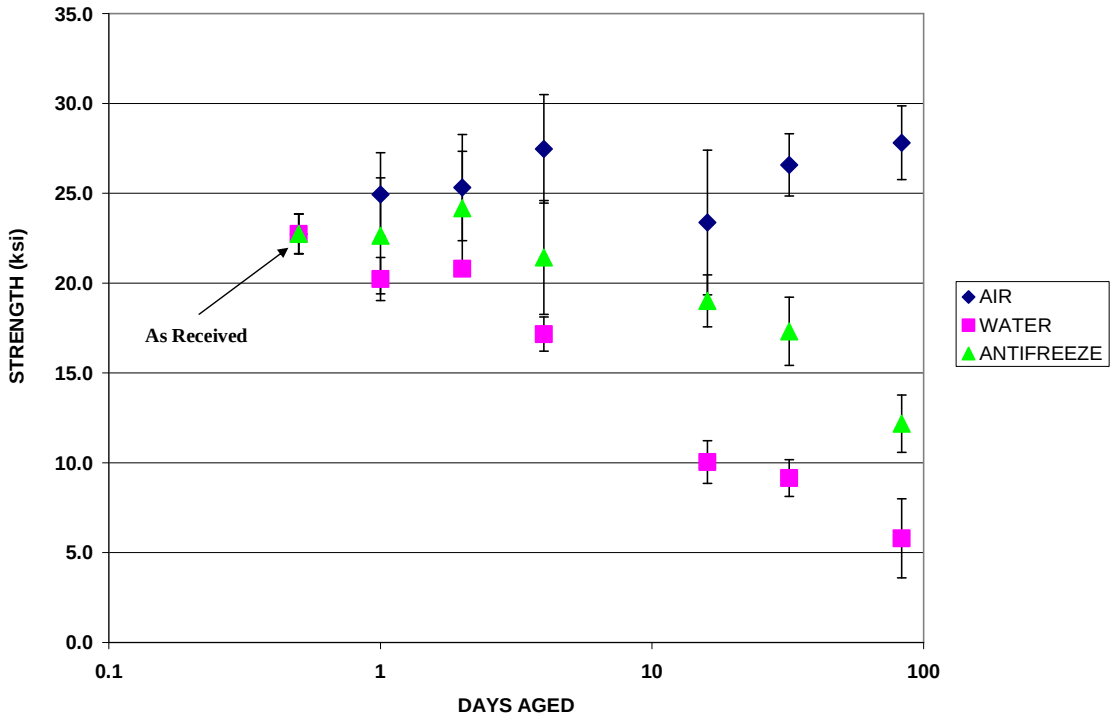

Figure 18: Materials B Tensile Strength vs. Aging Time

The increase in strength between the as received and 4 day tests are likely due to residual curing of the composite at the 85°C aging conditions. A dynamic mechanical analysis was conducted to determine if there was potential for additional curing and is shown in Figure 19. The increase in storage modulus between scan 1 and scan 2 is due to additional curing of the material. Aging in air at 85°C has little effect on the tensile strength of the Materials A material. This is not surprising considering the fibers and matrix are both very resilient at this temperature in dry conditions.

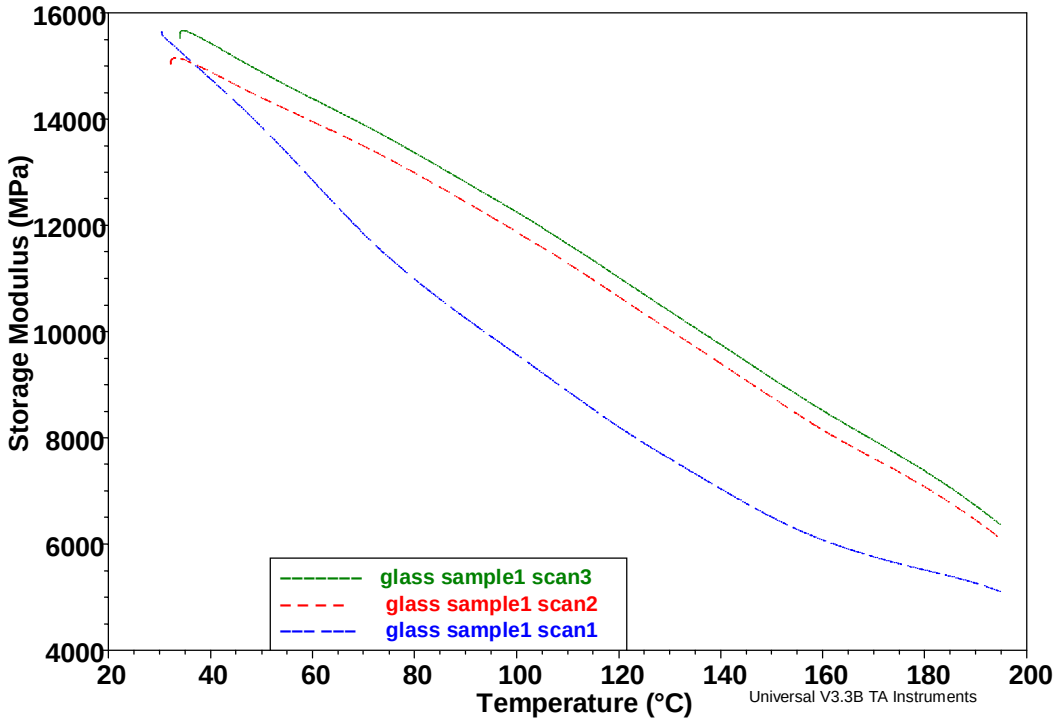

Figure 19: Dynamic Mechanical Analysis of Material B

The loss of strength of the Materials A and B materials aged in water and the 50/50 water/antifreeze mix is due to multiple factors. The first to consider is the likely reduction in the glass transition temperature of the matrix due to absorbed moisture. As stated earlier, moisture absorbed in epoxy acts as a plasticizer and reduces the glass transition temperature. This effect is likely the cause of the delamination and blistering seen in the samples exposed to water. In addition, as the process begins in the early stages of aging, the increased compliance of the material reduces the energy required for the water molecule to be transported into the free volume of the polymer. As the delamination begins, water quickly fills the free space and the damage continues eventually forming a water filled blister in the material. Aiding in the transport of water into these composites is the chopped fiber reinforcement. Composites with chopped fiber reinforcement are known to have greater diffusivities than their woven roving counterparts.

The additional loss in strength of the Materials B compared to the Materials A is likely due to damage to the glass fibers. With the high moisture content and the extreme moisture absorption mechanisms, the fibers and fiber matrix interfaces are highly vulnerable to water induced damage. The fiber damaged incurred is likely due to dissolution, selective leaching, and stress-corrosion cracking due to the exposure of the fiber to the absorbed water.

The effects of the lower concentration of water on the samples aged in the water/antifreeze mixture are apparent, especially in the Material B. Material B aged in the antifreeze mixture experienced an approximate strength loss of 50 percent. This same material aged in water lost nearly 75% of its original strength. While one would think the strength loss should be doubled because the concentration of water is doubled, there are several degradation mechanisms occurring simultaneously. What is important to note is that there is a preservation of strength by reducing the concentration of water and therefore the composites exposure.

The tensile data for Material B was compared with a known degradation model developed by Steve Phifer (soon to be published) for water aged glass reinforced polymers. The model is the double exponential relationship:

$$y = Ae^{(-x/B)} + Ce^{(-x/D)} \qquad \text{Equation 2}$$

where A, B, C, & D are fit perameters.
The comparison between the Materials B and this model are show in Figure 20 where A=55, B=7, C=46, and D=154.

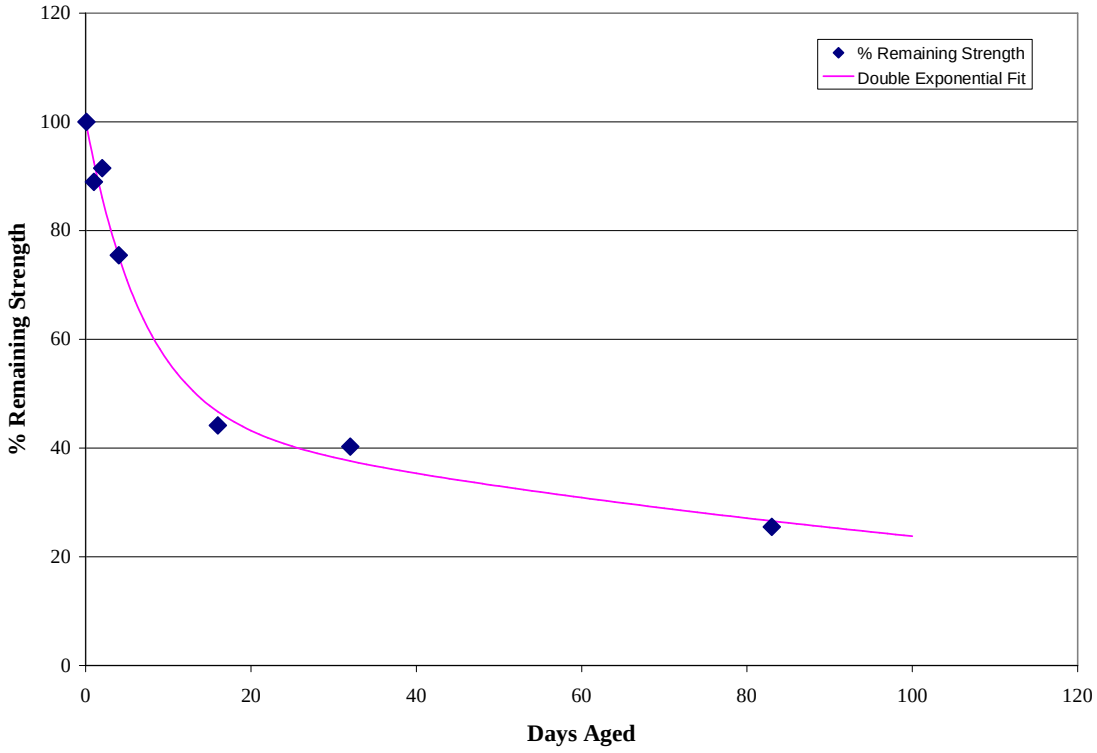

Figure 20: Double exponential fit for water aged Material B

In addition to loss in strength due to aging, a reduction in failure strain occurred for both Material A and Material B, as can be seen in Figure 21 and Figure 22 respectively. Water again appears to be the destructive component in the system. The fiber and matrix damage discussed above limits the elongation to failure of the composite. A weekend

matrix does not adequately transfer load following the fracture of a damaged or weakened fiber resulting in less elongation.

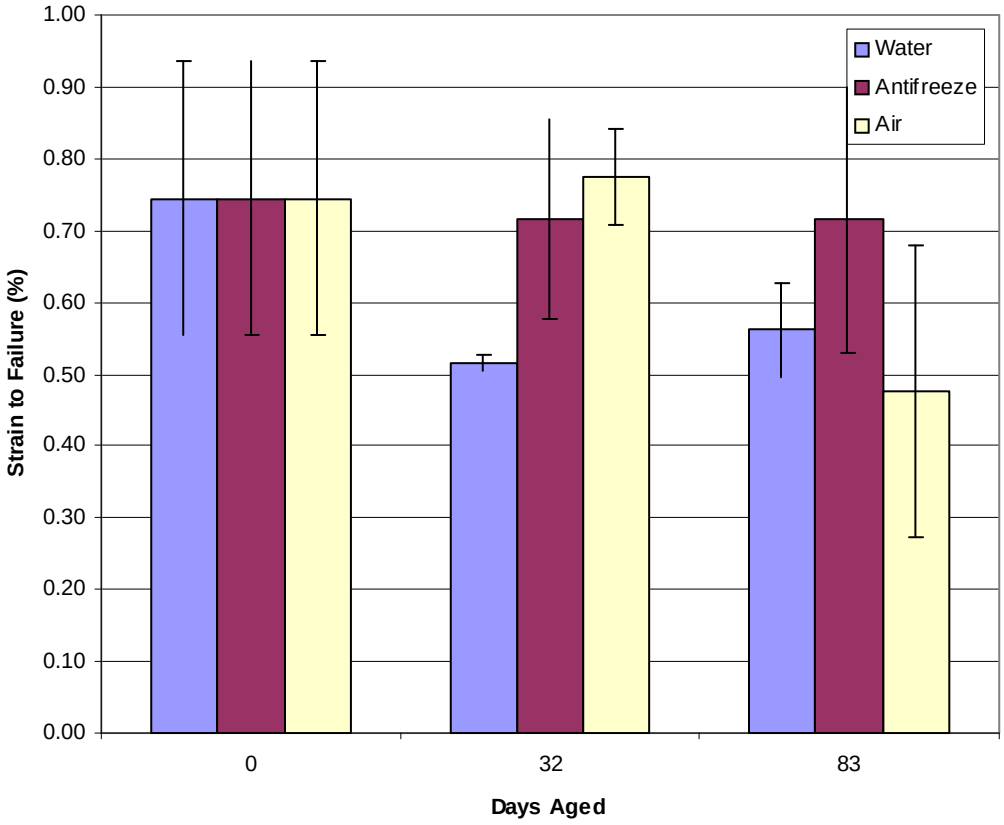

Figure 21: Percent strain to failure vs. Days aged for Material A

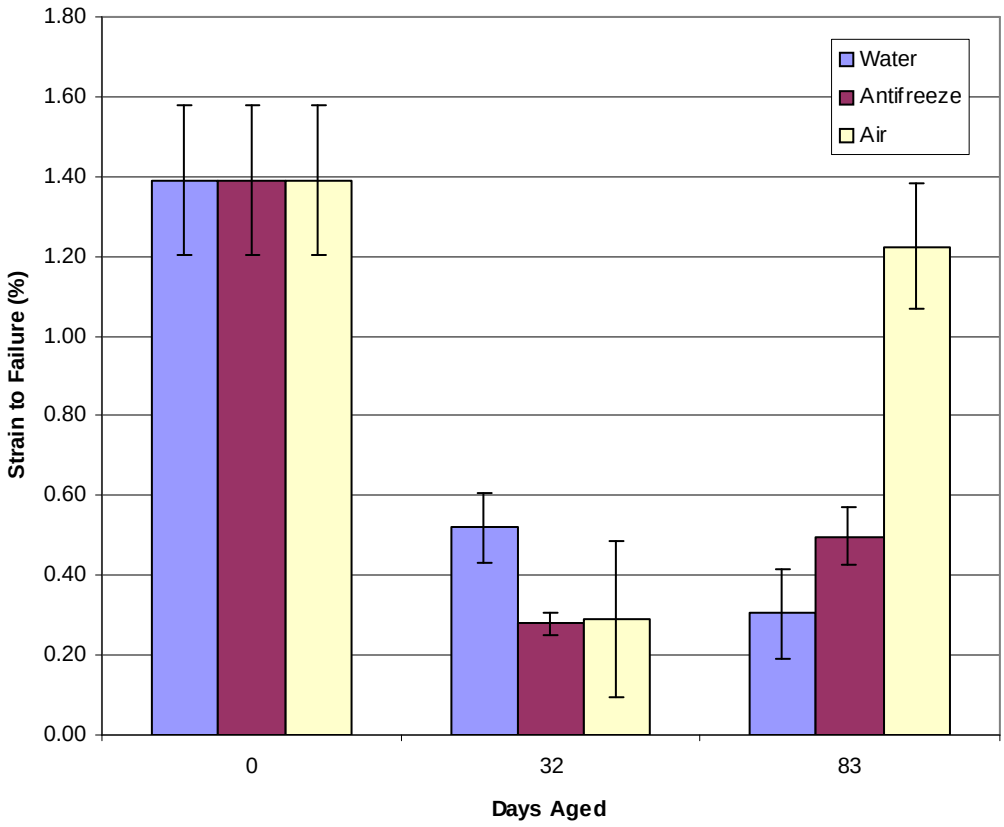

Figure 22: Percent strain to failure vs. Days aged for Material B

Significant variability may be present due the uncertainties associated with fiber alignment in a chopped fiber composite. Scatter in the data could be a function of the orientation of the fibers within a specific test sample or panel. Because of the panel construction method, it is likely that each panel and test sample have variations in fiber orientation distribution from the next.

3.2.2 Compression Testing

A set of five replicate quasi-static compression tests for each aging condition (air, water, 50/50 water/antifreeze mixture) were conducted for each of the composites of Material A and B for the as received, 1, 2, 4, 16, 32, and 83 days aged conditions. As can be seen in Figure 23, the typical failure mode is a V-shaped compression failure. This failure is consistent with efforts to prevent bending during compressive tests by using a gage section of 1.25 inches. Figure 24 and Figure 25 show the changes in average compression strength versus time for the Materials A and B materials respectively.

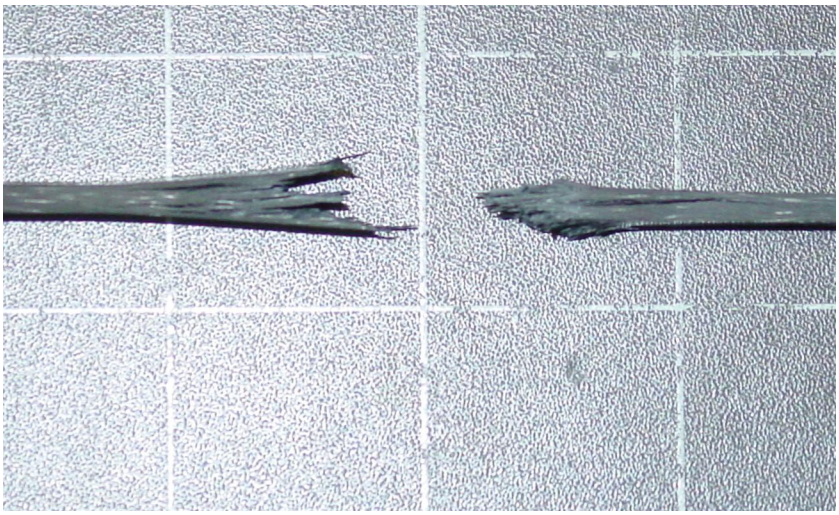

Figure 23: Typical compression failure.

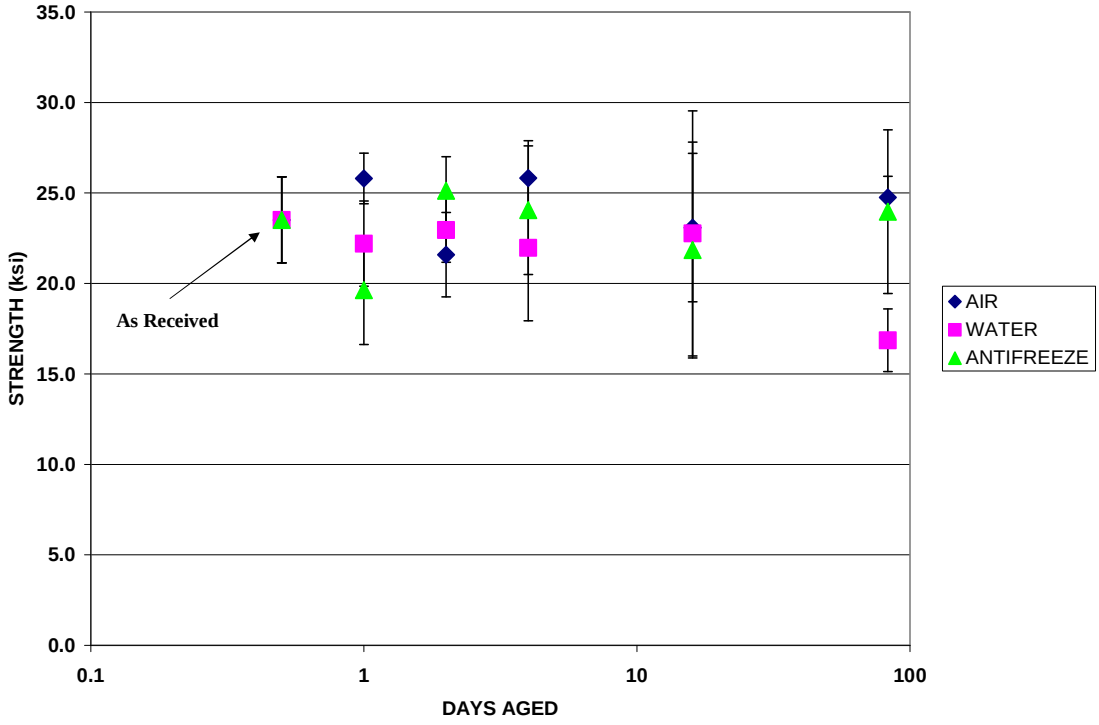

Figure 24: Material A Compression Strength vs. Time Aged

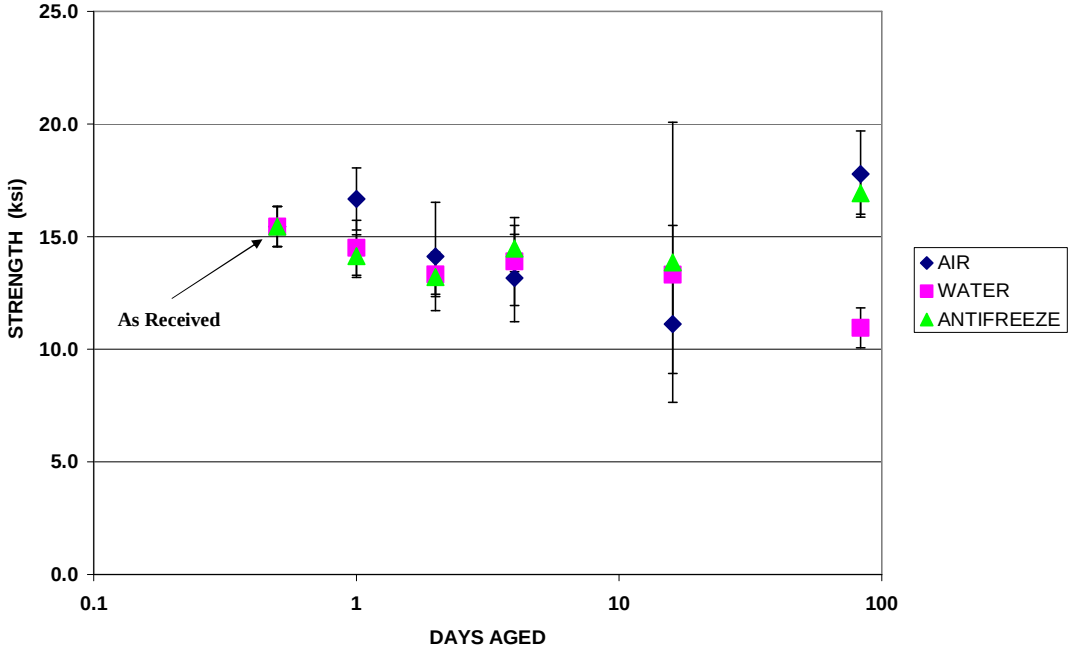

Figure 25: Material B Compression Strength vs. Time Aged

Though less defined then in the tensile case, the compression results show a reduction in strength over the aged timeframe. Greater strength loss is seen in the 83 day tests. This is due to the formation of blisters, as described above, in the water-aged specimens. The water-filled blisters change the shape of the composite forming a bend in the material. When loaded the blister-formed bend causes buckling and the composite fails. This mechanism can be referred to as delamination buckling. The process is illustrated in Figure 26.

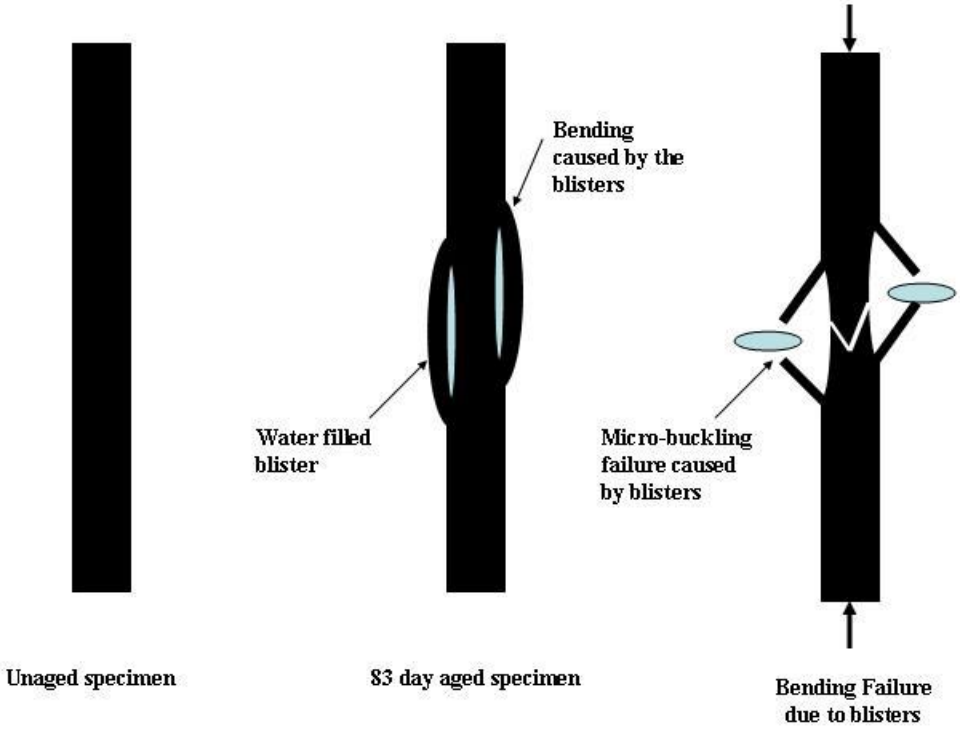

Figure 26: Micro-buckling Compression failure due to blister formation

3.3 Flexural Strength Testing

Flexural strength testing was conducted on both the Materials A and B for the as received condition and for the 83 day aged condition. Samples of both materials were aged in air, water, and the 50/50 water/antifreeze mixture. Flexural strength values are compared for Materials A and B for each aged condition in Figure 13 and figure 14 respectively.

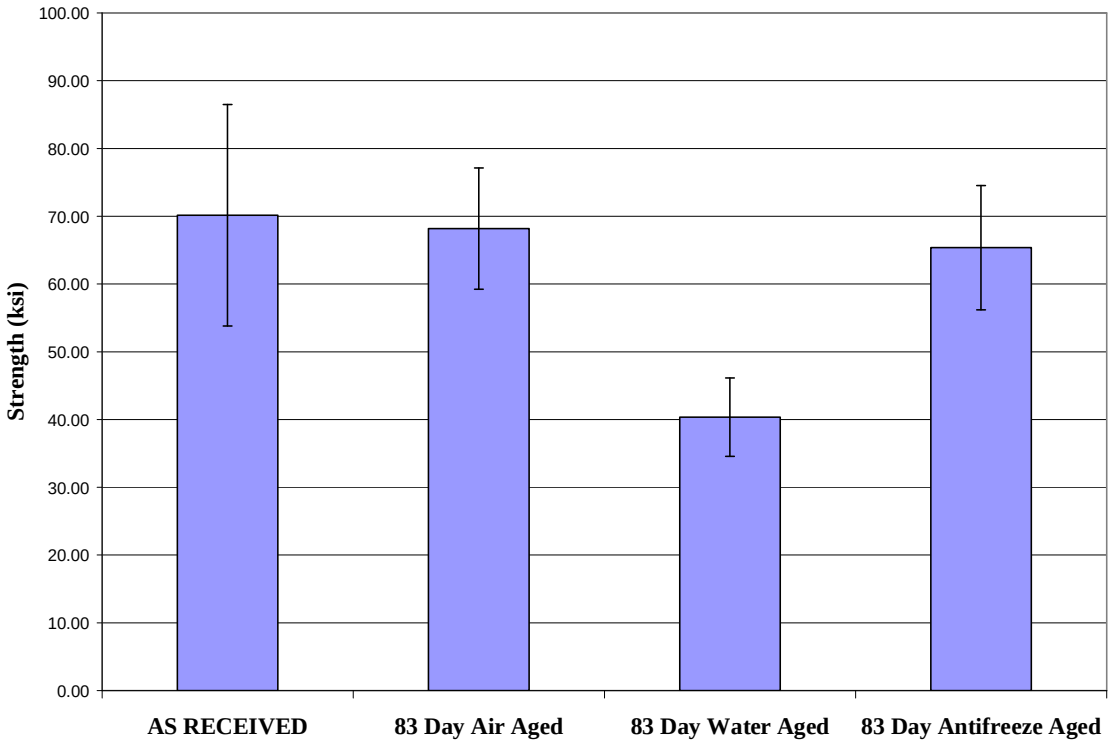

Figure 27: Flexural Strength of Material A

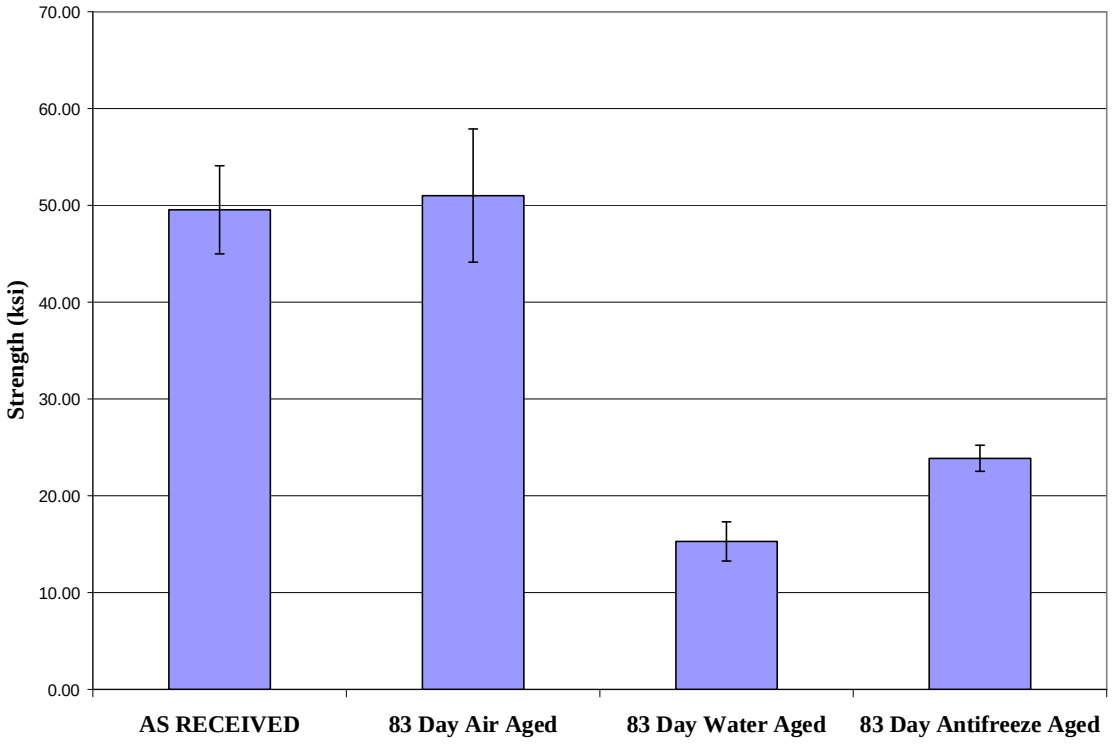

Figure 28: Flexural Strength of Material B

Water-induced damage is extremely prevalent in both materials. Aging in 85°C deionized water resulted in flexural strength reductions of approximately 40% for the Material A and 70% for the Material B. Both materials experienced the same matrix degradation described in detail earlier. Blister delamination prevents the load in the tensile section of bending sample from redistributed to subcritical elements. The result is fracture of the critical elements, which define the fracture of the composite at the global level [32]. For more information on the critical element theory, see Reifsnider and Case [32].

In addition, the greater flexural strength reductions in the Material B can be attributed to glass fiber degradation. The fiber damage incurred is likely due to dissolution, selective leaching, and stress-corrosion cracking due to the exposure of the fiber to the absorbed water.

3.4 Fatigue Testing

Mechanical fatigue testing was conducted and the mean stress effects were examined on as received samples of Materials A and B. The S/N curves were generated for each material at -20°C, room temperature, and 85°C; the S/N curves for Materials A and B at room temperature are shown in Figure 29 and Figure 30 respectively. Figure 31(Material A) and Figure 32 (Material B) shows the more developed S/N curves for the 85°C condition. The S/N curves developed for the -20°C condition are shown in Figure 33 and Figure 34.

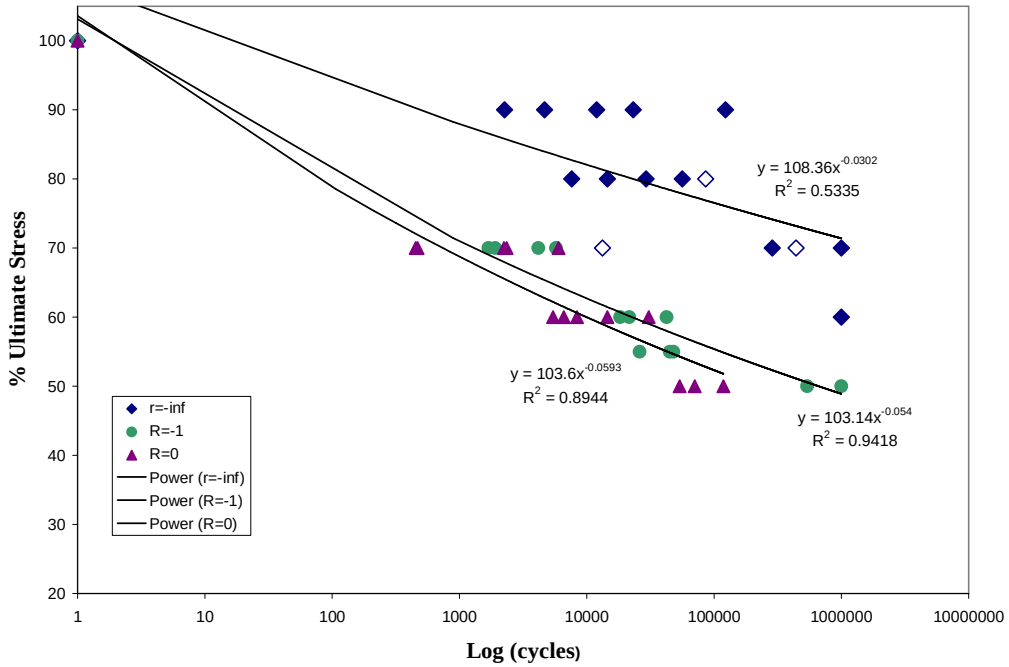

Figure 29: S/N Curve for Material A at room temperature

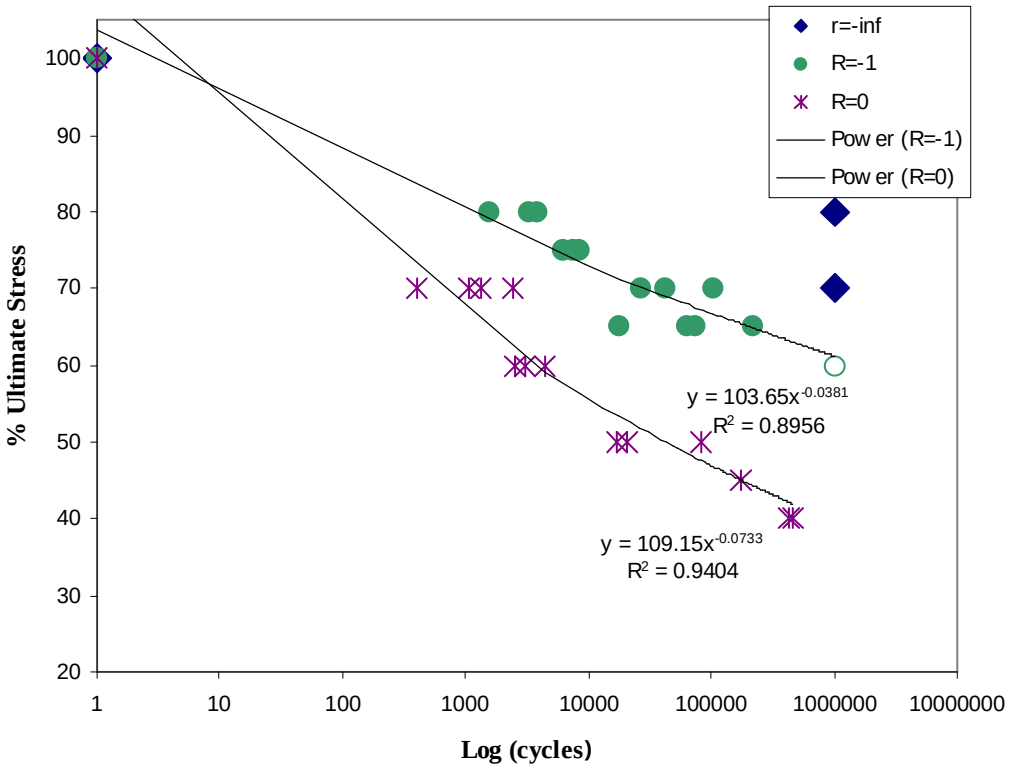

Figure 30: S/N Curve for Material B at room temperature

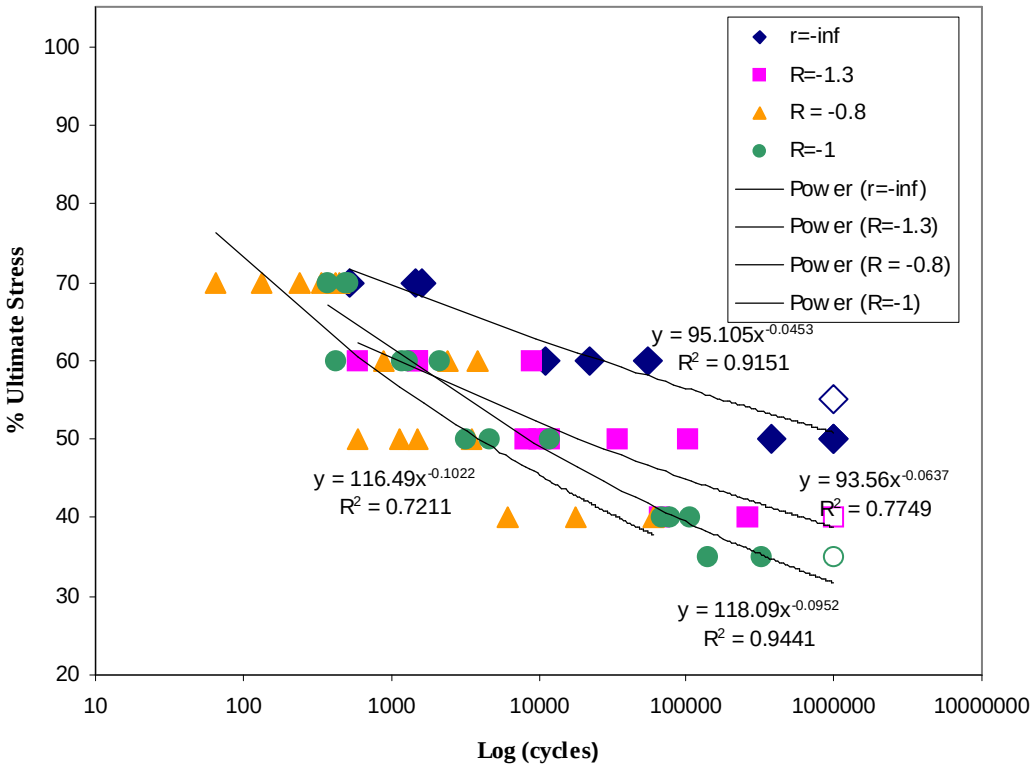

Figure 31: S/N Curve for Material A at 85°C

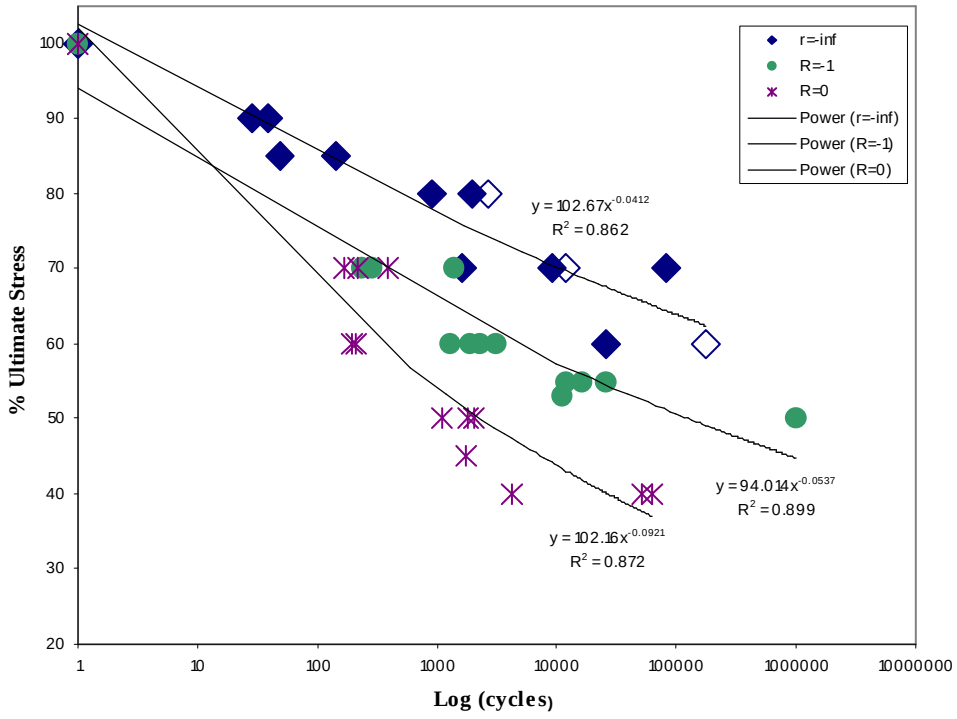

Figure 32: S/N Curve for Material B at 85°C

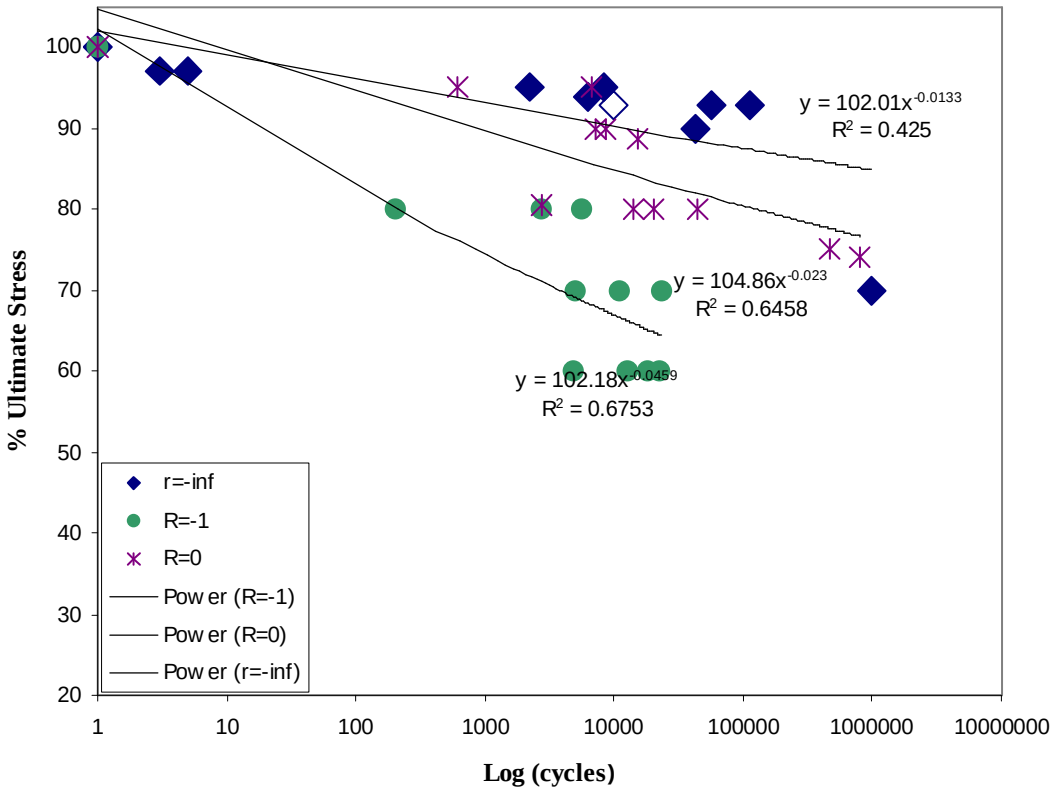

Figure 33: S/N Curve for Material A at -20°C

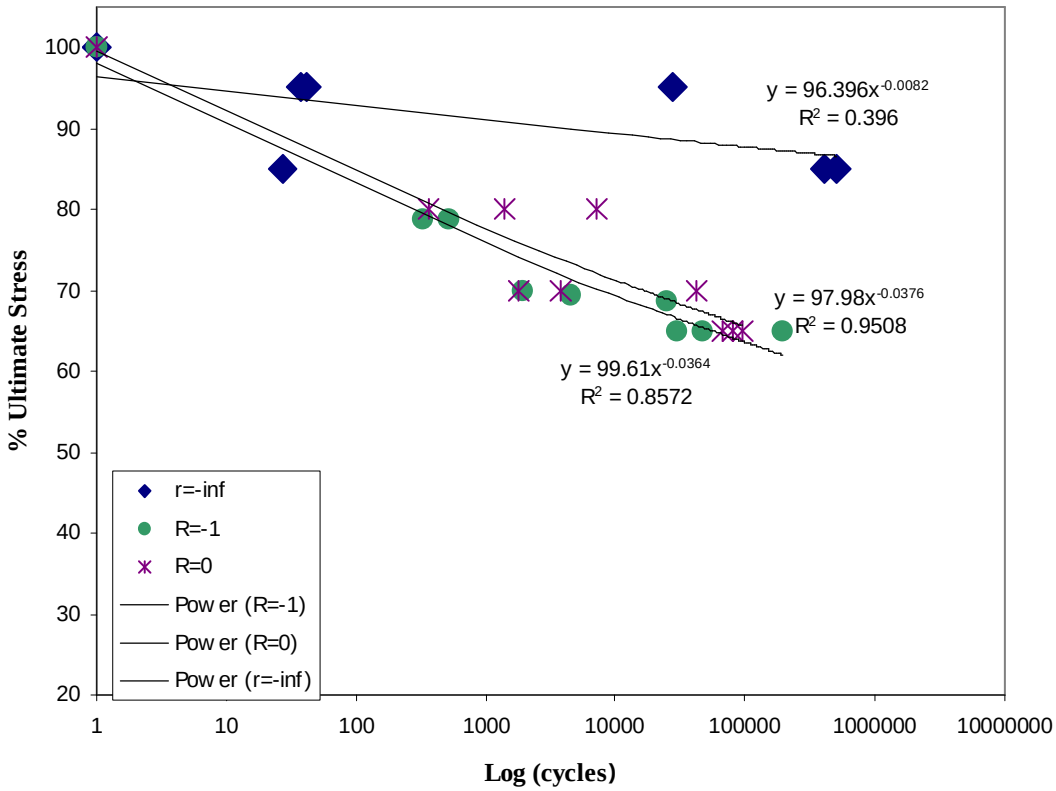

Figure 34: S/N Curve for Material B at -20°C

From the development of the S/N curves, fatigue lifetime plots were constructed. The fatigue lifetime plots compare the life of the material to the mean stress and amplitude stress. The fatigue lifetime plots for Material A and Material B for room temperature are shown in Figure 35 and Figure 36 respectively. The more developed 85°C fatigue lifetime plots are shown in Figure 37 (Material A) and Figure 38 (Material B). Figure 39 and Figure 40 show the fatigue lifetime plots for the -20°C test condition.

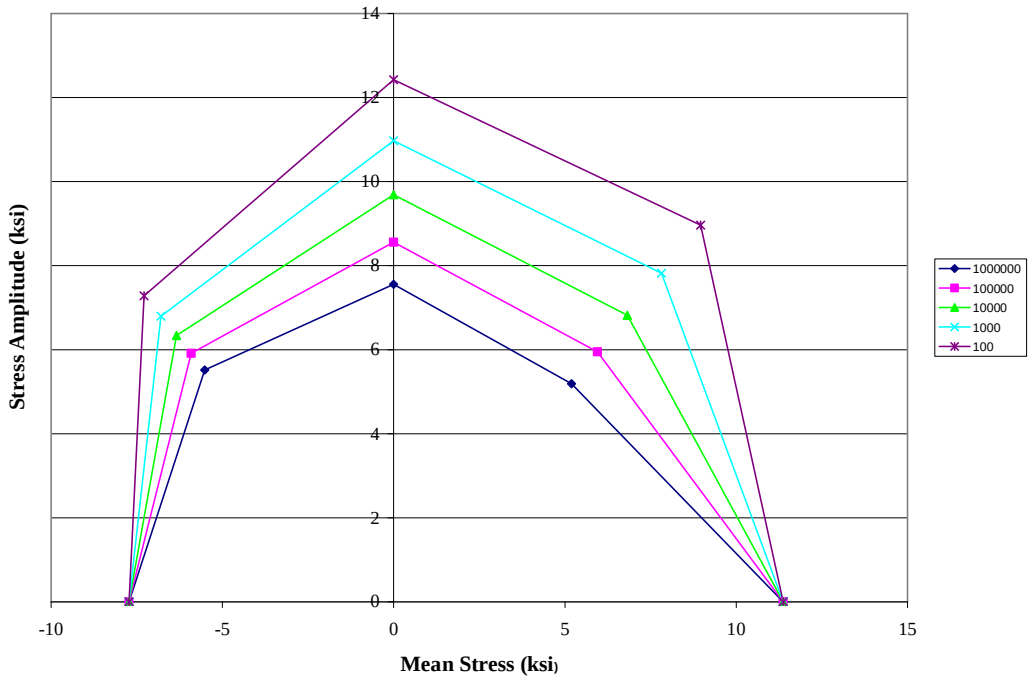

Figure 35: Room temperature fatigue lifetime plot for Material A

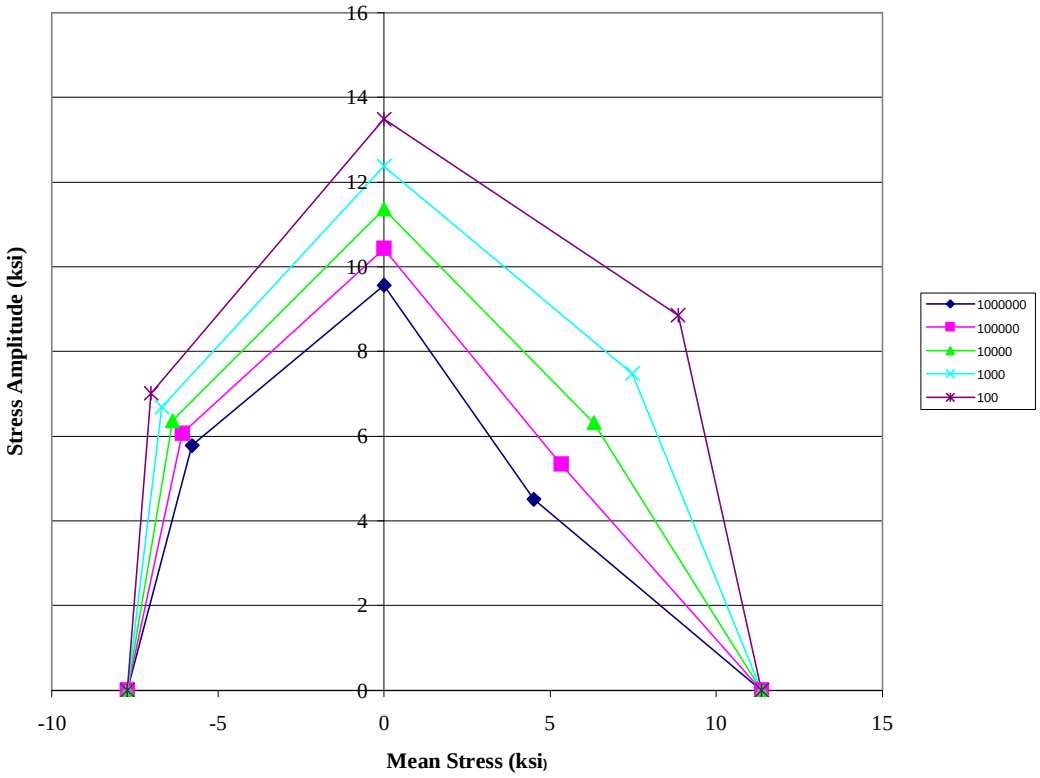

Figure 36: Room temperature fatigue lifetime plot for Material B

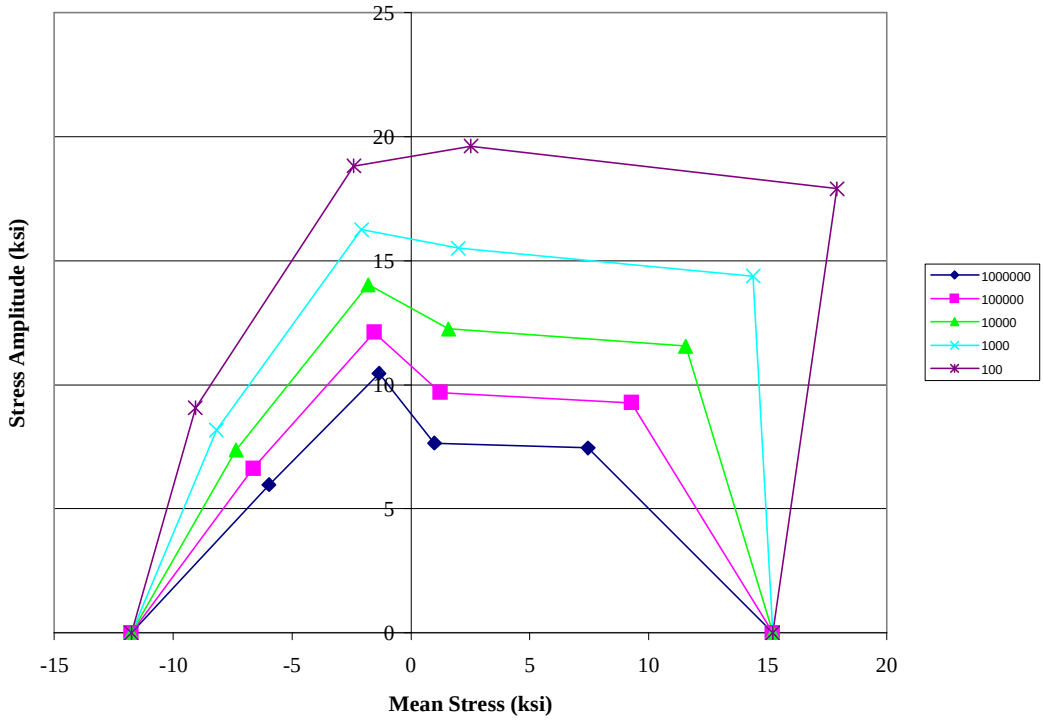

Figure 37: 85°C fatigue lifetime plot for Material A

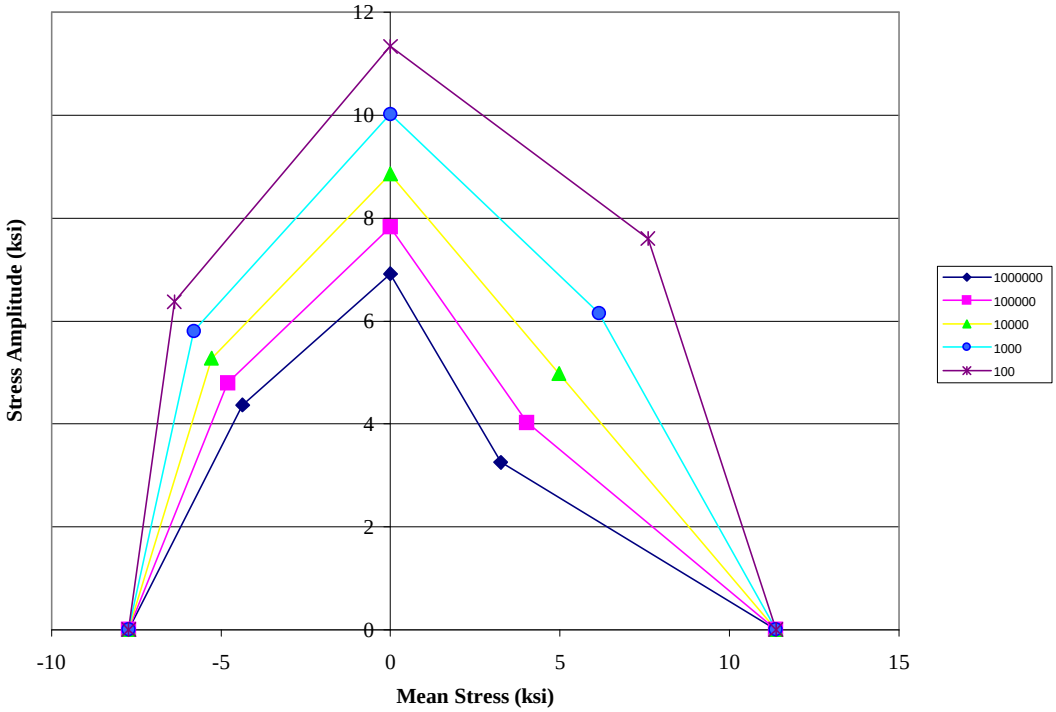

Figure 38: 85°C fatigue lifetime plot for Material B

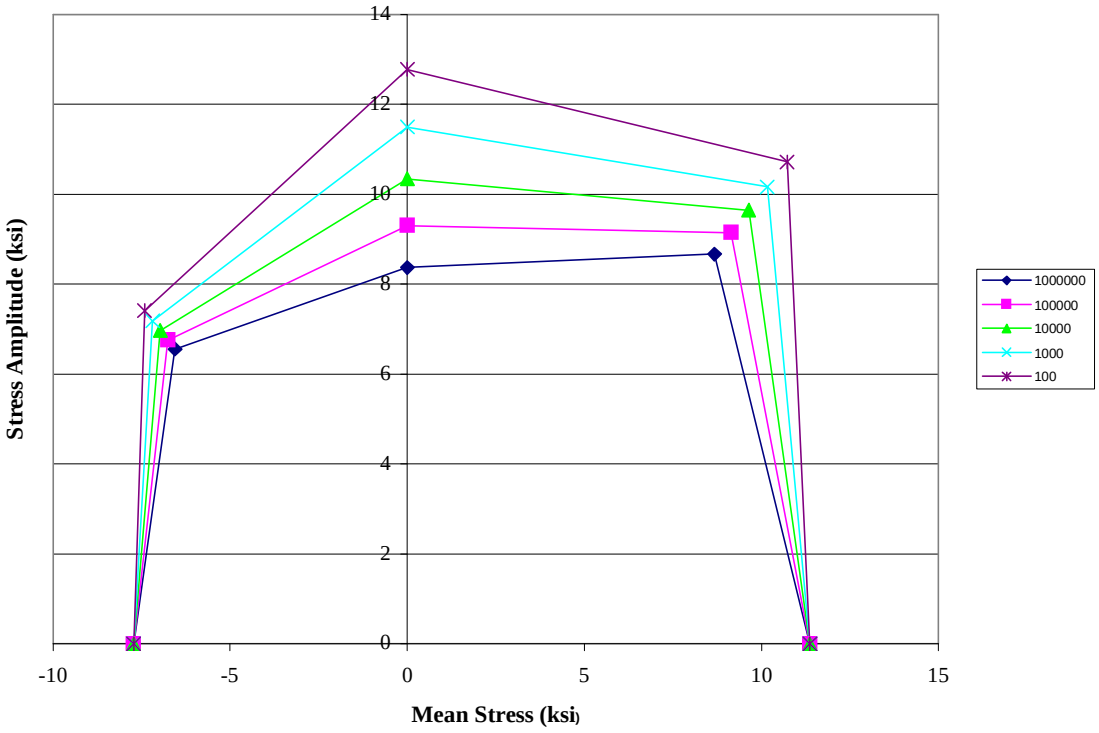

Figure 39: -20°C fatigue lifetime plot for Material A

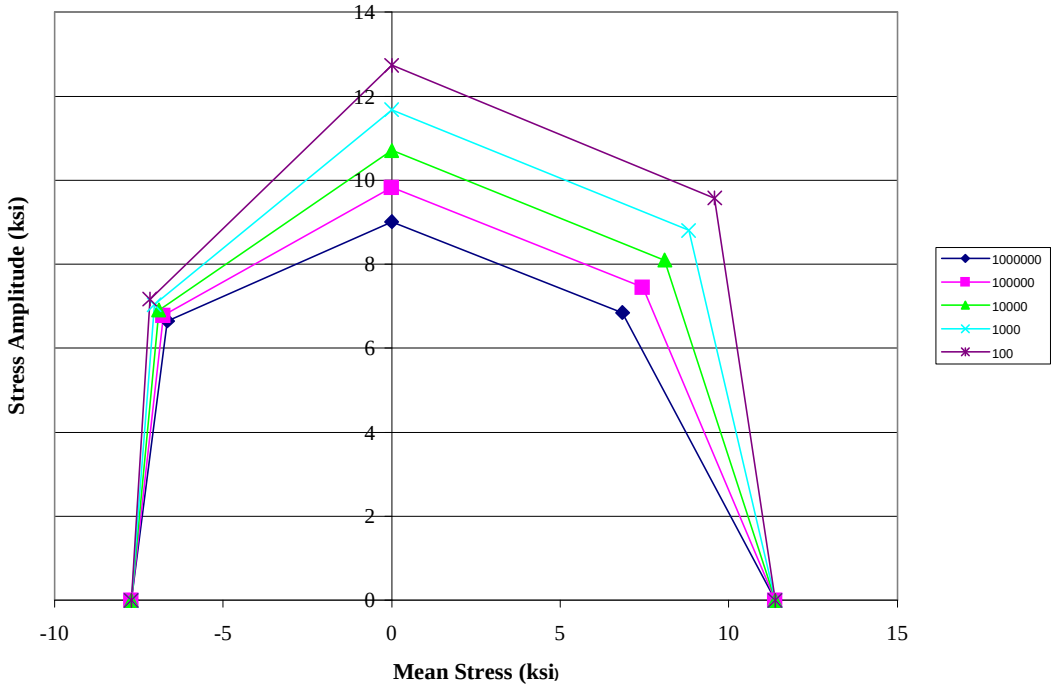

Figure 40: -20°C fatigue lifetime plot for Material B

Chapter 4: Conclusions & Recommendations

Based on the experimental data collected in this investigation, the following conclusions and recommendations were made:

- The moisture absorption for Material A and Material B was non-Fickian. This behavior is likely due to the delamination and blister formation, which permits a greater storage of unbound water within the composite. The mechanics of blister formation are complex. The likely mechanism for their formation begins with moisture absorption into the epoxy composite, which results in a reduction in the glass transition temperature. The absorbed water molecules interfere with the cross-linked structure of the epoxy through hydrogen bonding. This interaction between the water and the epoxy leads to micro-delaminations. With the reduction in glass transition temperature, the activation energy required for water penetration and interference hydrogen bonding is very low. The result is the propagation of water molecules at the delamination tip (crack tip), further penetration of water molecules, and further growth of the delamination into a water filled blister.

- The material degradation and delamination resulted in a tensile strength reduction of 25% for Material A and 70% for Material B for samples aged for 83 days in 85°C deionized water. Less of an effect was seen in the Material A aged in the 85°C antifreeze mixture, however the Material B lost approximately 45% of its tensile strength after 83 days of aging. The air-aged materials were unaffected or saw a slight gain in tensile strength likely due to post curing.

- The material degradation resulted in a reduction in strain to failure of 25% for Material A and 78% for Material B for samples aged for 83 days in 85°C deionized water. Less of an effect was seen in the Material A aged in the 85°C antifreeze mixture, however the Material B lost approximately 64% of its tensile strength after 83 days of aging. Although there was considerable scatter in the data, it is believed that stain to failure was unaffected for air-aged materials.

- The blistering due to water aging also affected the compression strength. The compressive strength of Material A was reduced by approximately 35%, and 31% for the Material B.

- Flexural strength testing was conducted on the as received materials as well as 83 day aged. Following 83 days of water aging, the flexural strength of Material A and Material B were reduced 42% and 70% respectively which is similar to the tensile results except the Material A saw greater loss of strength in the flexural test. For antifreeze aging, the Material A saw little effect, but the flexural strength of Material B was reduced approximately 50%, which is a similar to the tensile result. Air aging had little effect on either material.

- Fatigue lifetime plots were developed for both materials. These materials were tested in the as received condition. For Material A, the constant lifetime plots were fairly consistent for room temperature and –20°C fatigued samples. The

85°C constant lifetime plot shows a slightly greater lifetime for the material. This is likely due to possible residual curing during the fatigue cycle. There is little distinguishable difference in lifetime for Material B tested in the as received condition.

- Due to the nature of the degradation of these materials, several material changes and procedures are recommended. It is recommended that the structural fiber be changed from a chopped fiber to woven roving fibers. This increases the durability, reduces the material diffusivities and provides greater uniformity in the material. In addition, it is recommended that further experimentation to determine the optimal epoxy/hardener stoichiometry for the PEM fuel cell operating conditions. This limits the degradation of the matrix material greatly and provides greater stiffness for a given material density.

- Given the severe degradation of each of these materials after 83 days (2000 hours) of aging at 85°C, it is not recommended that this material be used for PEM fuel cell manifolds or pressure plates. In addition, further testing is recommended to determine the effects of pure antifreeze to determine if the water is the damaging component of the 50/50 mixture.

- If the chopped fiber composite is used for fuel cell manifold and pressure plate applications, it is highly recommended that the composite be protected in some manner to prevent interaction with moisture, thereby protecting it from the damage water may cause to the composite.

References

1. Larminie, James & Andrew Dick. *2000 Fuel Cell Systems Explained*, John Wiley & Sons, Ltd

2 . Image is owned and protected by Lynntech, Inc and was take from: "http://www.lynntech.com/images/Fuel%20Cell%20Fundamentals.gif" Accessed December 28, 2003

3 . Image is owned and protected by Ballard Power Systems AG and was take from: "http://www.sovereign-publications.com/ballard.htm" Accessed December 28, 2003

4. Office of Transportation Technologies, U.S. Department of Energy. "http://www.cartech.doe.gov/freedomcar/technical-goals.html#1" Accessed July 24, 2003

5. Energy Efficiencey and Renewable Energy, U.S. Department of Energy. http://www.eere.energy.gov/hydrogenandfuelcells/pdfs/national_h2_roadmap.pdf Accessed Dec 9, 2003.

6. Loos, Alfred. C. & George S. Springer. 1979. "Moisture Absorption of Graphite-Epoxy Composites Immersed in Liquids and in Humid Air," *Journal of Composite Materials*, Vol. 13, pp. 131-147

7. Bunker, B. C. 1994. "Melecular mechanisms for corrosion of silica and silicate glasses," *Journal of Non-Crystalline Solids.* Vol 179, pp. 300-308

8. Kohn, S. R. Dupree, & Me. E. Smith. 1989. *Nature*. Vol. 337 pp539

9. McKinnis, Charles L. "Stress Corrosion Mechanisms in E-Glass Fiber" *ASTM Symposium on Stress Corrosion*

10. Megel, M., L. Kumosa, T. Ely, D. Armentrout, & M. Kumosa. 2001. "Initiation of Stress-Corrosion Cracking in Unidirectional Glass/Polymer Composite Materials," *Composites Science and Technology*, Vol 61 pp 231-246

11. Medcalfe A. G. & G. K. Schmitz. 1972. "Mechanism of stress corrosion in E glass filaments," *Glass Technology*; Vol. 13, No 1, pp. 5-16

12. Charles, R. J., 1958, "Static Fatigue of Glass Part I and II," *Journal of Applied Physics*, Vol. 29, No. 11, pp. 1549-1560,1657-1663

13. Vanlandingham, M. R., R. F. Eduuljee, & J. W. Gillespie, Jr. 1999. “Moisture Diffusion in Epoxy Systems,” *Journal of Applied Polymer Science*, Vol 71, pp 789-798

14. Addamson, Michael J. 1980. “Thermal Expansion and Swelling of cured epoxy Resin used in Graphite/Epoxy Composite Materials,” Journal of Materials Science, Vol 15, pp 1736-1745

15. Zhou, Jiming & James P. Lucas. 1999. “Hygrothermal Effects of Epoxy Resin. Part I: The Nature of Epoxy in Water,” Polymer, Vol 40, pp 5505-5512

16. Zhou, Jiming & James P. Lucas. 1999. “Hygrothermal Effects of Epoxy Resin. Part II: Variations of Glass Transition Temperature,” Polymer, Vol. 40, pp. 5513-5522

17. Bradley, W. L. & T. S. Grant. 1995. “The Effect of the Moisture Absorption on the Interfacial Strength of Polymeric Matrix Composites,” *Journal of Materials Science*, Vol 30, pp. 5537-5542

18. McBagonluri, F., K. Garcia, M. Hayes, N. Verghese, & J. J. Lesko, 2000. "Characterization of Fatigue and Combined Environment on Durability Performance of Glass/Vinyl Ester Composite for Infrastructure Applications," *International Journal of Fatigue*, Vol. 22, Issue 1, pp. 53-64

19. Schultheisz, S. R., W. G. McCouough, S. Kondagunta, C. L. Schutte, K. S. Macturk, M. McAuliffe, & D. L. Hunston, 1997. “Effect of Moisture on E-Glass/Epoxy Interfacial and Fiber Strengths,” *Composite Materials: Testing and Design, Thirteenth Volume, ASTM STP 1242*, S. J. Hooper, Ed., American Society for testing and Materials, *pp. 257-286*

20. Singh, K. S., P. N. Singh, & R. M. V. G. K. Rao. 1991. “Hygrothermal Effects on Chopped Fibre/Woven Fabric Reinforced Epoxy Composites. Part A: Moisture Absorption Characteristics,” *Journal of Reinforced Plastics and Composites*, Vol. 10, pp. 446-462

21. Aditya, P. K. & P. K. Sinha, 1992. “Diffusion Coefficients of Polymeric Composites Subjected to Periodic Hygrothermal Exposure,” *Journal of Reinforced Plastics and Composite*, Vol. 11, pp. 1035-1047

22. Devine, F. E. 1983 “Polyester Moulding Materials in Automotive underbonnet Environments,” *Composites*, Vol 14, No. 4, pp. 353-358

23. Springer, G. S., J. A. Sanders, & R. W. Tung, 1980. “Environmental Effects on Glass Fiber Reinforced Polyester and Vinylester Composites,” *Journal of Compoiste Materials*, Vol. 14, pp. 213-232

24. Gupta, V. B., L. T. Drzal, C. Y-C. Lee, & M. J. Rich. 1985 "The Temperature – Dependance of Some Mechanical Properties of a Cured Epoxy Resin System," *Polymer Engineering and Science*, Vol. 25, No. 13, pp. 812-823

25. Zhou, Jiming & James P. Lucas. 1996. "Effects of Water on a Graphite/Epoxy Composite," *Journal of Thermoplastic Composite Materials*, Vol. 9, pp. 316-327

26. Skourlis, T. P. & R. L. McCullough, 1993. "The Effect of Temperature on The Behavior of The Interphase in Polymeric Composites," *Composites Science & Technology*, Vol. 49, No. 4, pp. 363-368

27. Ellyin, Fernand & Christof Rohrbacher, 2003. "The Influence of Aqueous Environment, Temperature and Cyclic Loading on Glass-Fibre/Epoxy Composite Laminates," *Journal of Reinforced Plastics and Composites*, Vol. 22, No. 7, pp. 615-636

28. Chiou, P. L. and W. L. Bradley, 1996. "Moisture-Induced Degradation fo Glass/Epoxy Filament-Wound Composite Tubes," *Journal of Thermoplastic Composite Materials*, Vol. 9, pp. 118-128

29. Jones, C.J., R. F. Dickson, T. Adam, H. Reiter, & B. Harris, 1983. "Environmental Fatigue of Reinforced Plastics," *Composites*, pp. 288-293

30. Grant, T. S. and W. L. Bradley, 1995. "In-situ Observation in SEM of Degradation of Graphite/Epoxy Composite Materials Due to Seawater Immersion," *Journal of Composite Materials*, Vol 29, No. 7, pp. 852-867

31. Quantum Composites High Performance Materials. "http://www.quantumcomposites.com/ESCsummary.pdf" Accessed July 08, 2003

32. Reifsnider, Kenneth L. & Scott W. Case, 2002. *Damage Tolerance and Durability of Materials System*, John Wiley & Sons, Inc., New York, pp. 86-87.